치의과학박사학위논문

Effects of bone marrow derived stem cells and PDGF/BMP-2 on the treatment of radiation induced skin ulcer and osteonecrosis in rats

백서에서 방사선조사에 의한 피부궤양과 골괴사 치료를 위한 골수유래 줄기세포와 PDGF/BMP-2의 적용 효과

2016년 2월

서울대학교 대학원

치의과학과 구강악안면외과학전공

진 임 건

Effects of bone marrow derived stem cells and PDGF/BMP-2 on the treatment of radiation induced skin ulcer and osteonecrosis in rats

백서에서 방사선조사에 의한 피부궤양과 골괴사 치료를 위한 골수유래 줄기세포와 PDGF/BMP-2의 적용 효과

지도교수 황 순 정

이 논문을 치의과학박사 학위논문으로 제출함

2015년 10월

서울대학교 대학원

치의과학과 구강악안면외과학전공

진 임 건

진임건의 박사학위논문을 인준함

2015년 12월

위 원 장 (인)

부위원장 (인)

위 원 (인)

위 원 (인)

위 원 (인)

Abstract

Effects of bone marrow derived stem cells and PDGF/BMP-2 on the treatment of radiation induced skin ulcer and osteonecrosis in rats

Jin Im Geon

Program in Oral and Maxillofacial Surgery, Department of Dental Science,

The Graduate School,

Seoul National University

(Directed by Professor Soon Jung Hwang, Dr. med. Dr. med. dent)

Background and Purpose

Osteoradionecrosis (ORN) of the mandible is a serious complication of radiation therapy, and it is preceded by soft tissue damage before bone loss appears. ORN is defined as a condition in which irradiated bone becomes exposed through a wound in the overlying skin or mucosa and persists without healing for 3 to 6 months. In the early stage of ORN, soft tissue necrosis occurs and is followed by exposure of bone tissue. As ORN proceeds, not only the exposed cortical bone but also

the underlying medullary bone undergoes necrosis, and eventually necrosis progresses to the lower body of the mandible. Because pathology of ORN was not understood clearly, a direct treatment modality has not been established for ORN. Since ORN begins from necrosis of soft tissue, delaying the speed of necrosis or improving the healing potential at this stage would minimize subsequent exposure of bone. After bone exposure, improvement of bony healing potential at the bony necrosis stage would also be beneficial in accelerating treatment of ORN. Recently, various effects of mesenchymal stem cells on wound healing have been reported. However, studies are lacking in the effect of application of mesenchymal stem cells or their combination with growth factors on healing of ORN at each stage.

This study investigated the effect of platelet derived growth factor (PDGF) or mesenchymal stem cells (rMSCs) on radiation-induced soft tissue injury and the effect of rat mesenchymal stem cells (rMSCs) or bone morphogenetic protein-2 (BMP-2) on the osseous healing of osteoradionecrosis in the rat mandible, depending on application time.

Part I. Effect on radiation induced soft tissue injury

[Materials and Methods] Sprague-Dawley rats (n=17) were

irradiated on the right and left buttocks with a single dose of 50 Gy. The right buttocks were administered with phosphate-buffered solution as a control. The left buttocks were administered with either rMSCs (2×10^6 cells), PDGF (8 μg), or PDGF combined with rMSCs. Administration was done at three weeks after irradiation. Wound healing was analyzed by calculating the percentage of residual ulcerated skin area compared to the total irradiated area during the five week healing period after administration. Modified skin scores were also assessed. Finally, skin lesions were histologically evaluated.

[Results]

More than 40% of the irradiated skin area within the irradiated zone underwent ulceration within 16 days postirradiation, with peak ulceration exceeding 50% around three weeks post-irradiation. Administration of rMSCs or PDGF alone did not confer any significant healing effect. The combined rMSCs+PDGF treatment significantly reduced the wound size compared with the nontreated control up to two weeks postinjection. Regarding the histological examination, lesions administered with PDGF (either alone or mixed with rMSCs) resulted in a greater deposition of highly organized collagen fibers throughout the dermis layer, compared with the control.

Part II. Effect on radiation induced bony necrosis

[Materials and Methods] The mandibles of SD rats were irradiated while sparing the body and internal organs by utilizing a non-occlusive skin clamp along with an x-ray image guided stereotactic irradiator. All wounds were created using the 30 Gy dose level on the right mandible at a 100 cm source-to-surface distance. One week after irradiation, all molar teeth on the right side of the mandible were extracted. Rats were randomly divided into two groups according to time of application of a hydrogel complex (n=25, each group). In Group 1, rMSCs and/or BMP-2 carried with hydrogel was applied immediate after surgery. In Group 2, it was done after the occurrence of ORN, four weeks after surgery. Micro-CT data of bone healing were compared among groups without hydrogel (n=5) and with hydrogel alone (n=5), or mixed with 2×10^4 of rMSCs (n = 5), or 10 μg of BMP-2 (n = 5), or both of them (n = 5). Animals without irradiation were used as the negative control.

[Results]

In Group 1, BMP-2 was effective in increasing both bone volume (BV) and bone mineral density (BMD), while rMSCs were not. All animals

showed ORN at irradiated areas in Group 2. In Group 2, the combined application of rMSCs and BMP-2 significantly increased BMD and BV compared to the groups without hydrogel and with hydrogel alone. BMP-2 application in Group 1 resulted in significantly higher BMD (6.29 ± 1.63%) compared to BMP-2 application in Group 2 (5.71 ± 0.94%).

Conclusions

The combined administration of rMSCs and PDGF efficiently enhanced the healing of radiation-induced skin ulceration. Osseous healing after post-irradiation trauma in rats was enhanced immediately after dentoalveolar trauma by application of BMP-2, while the combined application of rMSCs and BMP-2 was most effective after osteoradionecrosis occurred.

Key words: Mesenchymal stem cell, Platelet derived growth factor, Bone morphogenetic protein 2, Osteoradionecrosis, Rats

Student Number: 2012-30615

CONTENTS

INTRODUCTION AND REVIEW OF LITERATURE

Radiation therapy plays a major role in the treatment of oral and maxillofacial malignancies, either alone or in combination with surgery and/or chemotherapy. However, high doses of radiation can lead to unwanted side effects on the skeletal system, salivary glands, and overlying soft tissue of the maxillofacial area. Osteoradionecrosis (ORN) is one of the most frequent severe complications after radiation therapy, and is diagnosed when irradiated bone does not heal for more than three months (1). The incidence of ORN is reported as 3.5%–4.74%, and it can present clinically with various symptoms. The main clinical manifestation in the oral and maxillofacial area is an exposed necrotic bone with wound dehiscence or a fistula, though severe cases may include pathological fractures (2) (3).

The pathogenesis of ORN is not clearly understood. In 1983, Marx described ORN as a non-healing wound resulting from metabolic and tissue homeostatic disturbances (1). He pointed out that ORN is a non-healing state after irradiation trauma, and that infection is limited to the contaminated surface. In contrast, Store et al. demonstrated through DNA-DNA hybridization that the contaminated exposed bone surface is generally infected by bacteria, especially anaerobes, which

may play a fundamental role in the pathophysiology of ORN (4). Recently, Delanian S et al. suggested that ORN occurs through a radiation-induced fibro-atrophic mechanism (5). According to this theory, ORN follows a sequence of free radical formation, endothelial dysfunction, inflammation, microvascular thrombosis (leading to necrosis of microvessels and local ischemia), fibrosis, and remodeling, which finally lead to tissue necrosis. Thus, ORN can be seen as a decrease in healing activity at an irradiated site that progresses through impaired fibroblastic activity (6). To reach the tumor, the radiation waves need to penetrate the skin or mucosal layer; thus, radiation-induced soft tissue lesions are often unavoidable (7). The response of soft tissue to radiation is complex (8). The epidermis is damaged in the early stage of radiation, whereas later effects arise from insult to the dermal vasculature. One or two days after radiation exposure, temporary erythema appears, which is then followed by a more intensive erythematous reaction. Afterwards, dermal ischemia and dermal necrosis occur, resulting in soft tissue damage such as dermal atrophy and invasive fibrosis (9). In this way, response of soft tissue to radiation accelerates bony exposure.

Because the exact pathogenesis of ORN is unclear, a definitive treatment modality has not been established. Conventional treatment for radiation-induced soft tissue ulceration with superficial dressings requires a long healing period and frequently leaves residual lesions via atrophy, fibrosis, or bony exposure. This is especially true for long-term nonhealing ulcers that eventually require surgery (10). Conventional treatment is mostly based on symptomatic therapy, and consists of sequestrectomy, debridement, and surgical resection of the jaw bone, with or without defect reconstruction in severe cases, followed by meticulous wound closure (11). However, despite meticulous postoperative care, recurrent ORN is frequent and results from delayed wound healing and wound dehiscence with secondary infection, due to the reduced healing capacity after irradiation.

To overcome these disadvantages, a number of alternative treatments have been introduced (12-15). Among these alternatives, mesenchymal stem cells (MSCs) have shown the capacity to repair hard and soft tissue damage in animal models (16) and human patients (17, 18). With respect to their therapeutic effects on soft tissue damage, efficient results have been reported in animal models of lung injury (19), kidney injury (20), and myocardiac infarction (21). MSCs

produce various cytokines and adhesion molecules for hematopoiesis, and are known to participate in angiogenesis and wound repair (22). MSCs also express proangiogenic factors that regulate endothelial cell migration and capillary proliferation, and have been reported to be involved in vessel remodeling (23).

MSCs or growth factors can contribute to tissue regeneration in damaged tissue with an impaired healing capacity (24, 25), as seen in ORN (26). Bone marrow mesenchymal stromal cells had a therapeutic effect on ORN in a swine model (26). In another series of studies, MSCs were subcutaneously transplanted into immunocompromised mice, which led to the formation of organ-like structures including newly formed bone and associated hematopoietic marrow components (27-29).

Among the numerous identified growth factors, platelet-derived growth factor (PDGF) is considered particularly critical for vascular formation. The homodimer PDGF-BB responds to hypoxia, growth factors, and shear stress and is expressed highly at the sprouting tip of forming capillaries, where it contributes to pericyte recruitment (30). PDGF-BB also stimulates pericyte production of extracellular matrix proteins, including fibronectin, collagen, and proteoglycans,

which are necessary for the basement membrane of capillaries. In addition, PDGF-BB upregulates the expression of vascular endothelial growth factor (VEGF) in mural cells and stimulates fibroblasts to produce and secrete collagenases, which are key for cell migration in angiogenesis (31).

Bone morphogenic protein-2 (BMP-2) is regarded as the most potent growth factor for bone regeneration (32-34). It may be also effective for tissue repair in ORN, as predictable bone generation was seen after the application of BMP-2 in a rat mandible ORN model (25). Animal ORN models have shown that inhibition of endogenous BMP-2 and osteocalcin (35). Therefore, exogenous BMP-2 should be able to enhance osseous regeneration in ORN. This exogenous BMP-2 and MSC therapy should be applied at the optimal time, where these substitutes can act most effectively to repair tissue. However, it is unclear whether the best time of administration is immediately after tissue damage (e.g., tooth extraction) or after occurrence of pathologic status (e.g., ORN).

Even though a synergic regeneration efficacy can be expected with a combination of MSCs and PDGF/BMP-2, the effect of combined therapy in the ORN model has not been investigated. The purpose of

this study was to investigate the effect of MSCs and/or PDGF alone for treating radiation-induced soft tissue injury and the effect of MSCs and BMP-2 on the osseous healing of ORN in the rat mandible at two different administration times.

PART I. EFFECT ON RADIATION INDUCED SOFT TISSUE INJURY

A. Materials and methods

1. Animal model of radiation-induced skin ulceration

All animals in these studies(part I and part II) were treated and handled in accordance with the "Recommendations for Handling of Laboratory Animals for Biomedical Research" compiled by the Committee on the Safety and Ethical Handling Regulations for Laboratory Experiments at the School of Dentistry, Seoul National University.

Adult male Sprague-Dawley (SD) rats (n=18; mean mass, 120 g)

(Orientbio Inc. Seongnam. Korea) were irradiated on both buttocks at six weeks of age. For each animal, the left buttock was assigned as the experimental side and the right buttock was assigned as the control side. After intraperitoneal injection of Zoletil 50 (0.1 mg/100 g) (Virbac, Paris, France), the buttocks of each rat were shaved and prepared with povidone-iodine solution (MEDICA KOREA, Seoul, Korea). Rats were irradiated with a single electron beam delivered by a Clinac iX linear accelerator (Varian Medical System, Inc., Palo Alto, CA, USA). The total irradiated area for each buttock was 3.5 cm x 3.5 cm = 12.25 cm^2. A 3-mm lead filter was added to the skin site to remove low energy photons from the beam at a 100 cm source-to-surface distance. Radiation (50 Gy, 6 MeV electron, 5501 MU) was delivered to 3.5 cm x 3.5 cm areas on the skin (depth range, 2 mm) of both buttocks. Rats were housed individually to prevent gnawing of wounds and other potentially damaging interactions.

2. Preparation and culture of rMSCs

Bone marrow aspirate was obtained from rat tibias. Rat MSCs were cultured according to the protocol described by Caterson et al. (36). Briefly, the marrow suspension was collected in a syringe containing

6000 U/mL heparin (JW Pharmaceutical Co., Seoul, Korea), mixed with an equal volume of phosphate-buffered solution (PBS) (Gibco, Rockville, MD, USA), and spun by centrifugation at 2500 rpm for 10 min. After aspirating the upper PBS layer, the marrow suspension was layered onto Ficoll-Paque (1:5 ratio) (GEHealthcare Life Sciences, Piscataway, NJ, USA) and spun by centrifugation at 2580 rpm for 30 min. Nucleated cells, which concentrated at the interface, were collected and washed with PBS. Adherent cells were plated at a density of 2 x 10^6 cells/100 mm dish and cultured in expansion medium containing alpha-MEM (Welgene Inc., Gyeongsan, Korea), 100 units/mL penicillin (Gibco, Rockville, MD, USA), 100 μg/mL streptomycin (Gibco, Rockville, MD, USA), and 10% heat inactivated FBS (HIFBS) (Gibco, Rockville, MD, USA) under a humidified atmosphere of 5% CO_2 at 37℃. Culture medium was changed every 3 or 4 days. rMSCs were passaged upon reaching 70% confluence. All experiments were performed using cells in their fifth passage.

3. Flow cytometry

rMSCs in their fifth passage were resuspended in phosphate-buffered saline (PBS) at 1x10^5 cells/mL and then incubated with

fluorescein isothiocyanate (FITC)-conjugated monoclonal antibodies against CD90 (LifeSpan Biosciences Inc., Seattle, WA, USA) or CD45 (LifeSpan Biosciences Inc.), each diluted to 1:200 in PBS. Alternatively, cells were incubated with anti-mouse IgG (BD Biosciences, San Jose, CA, USA) as an isotype control. Cells were incubated for 30 or 90 min in the dark after being washed with 1% bovine serum albumin in PBS (BSA/PBS). Cells were washed twice with BSA/PBS and resuspended in BSA/PBS with 0.1% paraformaldehyde (Sigma-Aldrich, St. Louis, MO, USA) for fluorescence-activated cell sorting (FACS) analysis. Cells were then fixed in 70% alcohol and sorted using a BD FACS Aria Cell Sorting System (BD Biosciences, San Jose, CA, USA).

4. Application of rMSCs and PDGF

Throughout the study, identical doses of rMSCs and/or PDGF were used in all groups. Moreover, the cell density also remained constant among the groups ($1x10^6$ rMSCs/cm^2), which has been shown to be adequate for effective tissue regeneration (12). rMSCs and PDGF were applied three weeks after irradiation, identical amounts of rMSCs ($2x10^6$ cells/2ml) and PDGF (8 μg) were evenly injected

subcutaneously over the entire ulcerative skin lesion, which varied in location and size (Figure 1(a)). For rMSC delivery, 1 mL of rMSC suspension ($1x10^6$ cells/ml in PBS) was filled in 1 ml syringe and total 2 syringes of rMSCs were injected subcutaneously at each site. As a control, 1 mL PBS was injected into each site on the control side.

Animal study only included animals for which the radiation-induced ulcers on the experimental side and control side did not exhibit any significant differences in size at three weeks after irradiation. One rat was excluded because its ulceration ratios were significantly different between the control and experimental sides (24.04 % vs 50.24 %). Animals (n=17) was subdivided into three groups: Group A: rMSCs (n=6), Group B: PDGF (n=6), and Group C: rMSCs+PDGF (n=5). Skin ulcers were measured over a five-week healing period after the administration of rMSCs and/or PDGF. Five weeks after treatment, skin samples were evaluated histologically by hematoxylin and eosin (H&E) staining and Masson's trichrome (MT) staining. To verify the presence of the delivered rMSCs, two rats were injected with fluorescent dye-labeled rMSCs at three weeks post-irradiation. The rats were sacrificed on the 3^{rd} and 7^{th} days postinjection, respectively, and the presence of the delivered rMSCs was verified. These two rats

were excluded from statistical analysis.

5. Wound model and wound healing assay

Acute skin reactions were assessed by visual scoring 21 days after irradiation. Assessment continued every three days until 35 days postinjection. Skin reactions were scored at each time point; data are presented as means. For scoring, the modified skin score system was used as follows: 0, normal; 0.5, slight epilation; 1.0, epilation in approximately 50% of the irradiated area; 1.5, epilation in more than 50% of the area; 2.0, complete epilation; 2.5, dry desquamation in more than 50% of the area, 3.0, moist desquamation in a small area; and 3.5, moist desquamation in most of the area (37).

For wound size analysis, the irradiated area of each rat was photographed with a digital camera at each time point. From these images, the percentage of the ulcerated area was determined by calculating the ratio of the ulcerated area to the total irradiated area using ImageJ, version 1.47 (NIH, Bethesda, MD, USA) (Figure 1(b)). The total irradiated area and ulcerated area were marked three times while blinded to the group assignments, and the average values of

these measurements were used for assessment. The irradiated area was defined as the area in which hair loss was observe (37). The ulcerated area was defined by scabbing, crusting, or desquamation. The numbers of pixels within each zone were calculated using ImageJ, and these values were used to calculate the percentage of skin ulceration within the irradiated zone.

6. Histological examination

Samples were fixed in 10 % formalin-buffered solution (Duksan Pure Chemicals Co. Ansan-si. Korea) and embedded in paraffin wax (Leica Biosystems Nussloch GmbH, Nußloch, Germany). For histochemical staining, the paraffin sections were cleaned with xylene (Duksan Pure Chemicals Co. Ansan-si. Korea) for ten minutes. Next, four-μm-thick slices were prepared and stained with both Hematoxyline and Eosin (H&E) (Sigma-Aldrich, St. Louis, MO, USA) and Masson's trichrome (MT) (Sigma-Aldrich, St. Louis, MO, USA). Digital images of the stained sections were captured for histological evaluation using a transmission and polarized light Olympus BX51 Axioskop microscope (Olympus Corp., Tokyo, Japan). Skin damage in the affected areas (epidermal atrophy, number of lymphocytes, dermal

degeneration such as edema and collagen fiber loss) is expressed as percentages. Skin damage was scored on a 5-point ordinal scale as previously described (14, 38): Grade 0 = normal, Grade 1 = minimal, Grade 2 = mild, Grade 3 = moderate, Grade 4 = marked, and Grade 5 = severe.

7. Labeling of rMSCs with dialkylcarbocyanine

rMSCs were labeled with the fluorescent dye dialkylcarbocyanine (Dil; Molecular Probes®, Thermo Fisher Scientific Inc., Waltham, MA, USA) by incubating cells in medium containing Dil (final concentration 10 ng/mL) for 24 hours. Dil-labeled rMSCs were injected subcutaneously into the left side of the irradiated buttocks of two rats. Histological specimens were prepared after sacrifice at three and seven days postinjection as described above, and the presence of rMSCs was verified using a confocal laser scanning microscope (Carl Zeiss Micro Imaging GmbH, Jena, Germany). To investigate the viability of rMSCs, the expression of proliferating cell nuclear antigen (PCNA) was verified.

8. Statistical analysis

All wound healing data are reported as means ± standard deviations. Data were checked for a normal distribution using the Kolmogorov–Smirnov test. When data were normally distributed, the experimental side was compared with the corresponding control side using a paired *t*–test. Data with non–normal distributions were compared using the Wilcoxon signed–rank test. All statistical analyses were performed with SPSS (ver. 18.0, SPSS, Chicago, IL, USA). Differences between values were considered statistically significant when the *p*–value was <0.05.

B. Results

As shown in Fig. 2, CD45 and CD90 could be detected by flow cytometric analysis. No systemic or lethal sequelae occurred in any animal. Moreover, no recognizable changes were observed on the irradiated skin until one week postirradiation. The first observable change was hair loss at 7 days postirradiation; ulcerative skin changes

were first seen at 10 days postirradiation. By day 14, necrotic changes were observed throughout the entire skin layer of the irradiated area. Peak ulcer size was observed on the 21st day postirradiation. Ulcerative lesions occurred independently of the injection site after irradiation and varied in location, size, and shape.

The modified skin scores were ranged from 3 to 3.5 at the time of injection on both the experimental and control sides of each animal; these scores decreased to 2 – 2.5 according to the follow-up period (Figure 3, Table 1). In Groups A and B, the scores decreased to 3.0 after 7-8 days, with no significant difference between the experimental and control sides. In Group C, the scores decreased to 3.0 after only 2 days; however, no significant difference was observed between the experimental and control sides (Figure 3).

1. Ulceration size evaluation

rMSCs alone or PDGF alone did not markedly enhance macroscopic healing of the radiation-induced skin wound, while rMSCs+PDGF treatment significantly aided the early stage of wound healing. In Group A, the ulceration ratios at the time of injection were 38.51 ± 10.74% on the experimental side and 41.60 ± 7.78% on the control side. Ulcer size decreased significantly during the first two weeks

postinjection on both sides, whereas the reduction rate decreased after this time. However, the ulceration ratio on the experimental side was not significantly different compared with the ratio on the control side. If anything, the ratio tended to be smaller on the control side. At five weeks postinjection, the average ulcerative lesion size on the experimental side was 1.37 ± 0.73%, and two out of the six rats showed no ulcerative skin lesions at all. The ulceration ratio on the control side was 0.82 ± 0.97%; all six rats exhibited ulcerative lesions on the control side (Figure 4(a), Table 2).

In Group B, the ulceration ratios at the time of injection were not significantly different (50.22 ± 5.10% on the experimental side vs. 45.11 ± 6.78% on the control side). The ulceration ratios decreased over time. As in Group A, ulcer size decreased most dramatically during the first two weeks after the injection, after which the reduction rate decreased. However, no significant difference was observed between the both experimental and control sides at five weeks postinjection. At this time, four out of the six rats showed ulceration on the experimental side, while two out of the six rats showed ulceration on the control side (Figure 4(b), Table 2).

In Group C, the ulceration ratios were also not significantly different

at the time of injection (44.40 ± 7.54% on the experimental side vs. 46.39 ± 12.54% on the control side, Figure 4(c), Table 2). However, the two sides did exhibit significant differences in healing after treatment. Three days after treatment, the ratios were 31.56 ± 14.03% and 35.79 ± 13.11% on the experimental and control sides, respectively (p=0.015). At seven days postinjection, the difference between the two sides had decreased (25.00 ± 10.49% vs 26.57 ± 10.54% on the experimental and control sides, respectively; p=0.045). At ten days, the ulceration ratio was still significantly smaller on the experimental side (18.58 ± 11.45%) than the control side (20.60 ± 10.30%) (p=0.004). Two weeks after the injection, however, no significant difference was observed (18.20 ± 13.46% vs. 17.21 ± 10.94%) (Figure 5). At five weeks postinjection, two of the five rats exhibited ulceration on the experimental side, while five of the six rats showed ulceration on the control side.

2. Histological examination

Histological examination of the skin ulcers was performed at five weeks postinjection. All three treatments (rMSCs alone, PDGF alone, and rMSCs+PDGF) resulted in positive microscopic effects on wound

healing. In Group A, erosion of the epidermis layer was observed in 43.99 ± 15.20% of the control skin area, and edema (Grade 3-4) was present in all specimens. In contrast, the experimental side of Group A tended to show less erosion of the epidermis layer (25.00 ± 16.42%). Moreover, edema was observed in half of the experimental specimens (3/6) and the edema intensity was less (Grade 2) compared with the control side (Figure 6(a), 6(b)). In Group B, the epidermis layer showed erosion in 33.33 ± 22.51% of the control area, and edema (Grade 3) was present in five out of the six rats. In contrast, the experimental side showed less erosion of the epidermis layer (15.00 ± 17.61%), and edema (Grade 2-3) was present in four out of the six rats. In Group C, the control side showed erosion in 48.61 ± 21.05% of the epidermis layer, and edema (Grade 3-4) was present in all six animals. The experimental side tended to show less erosion of the epidermis layer (37.18 ± 23.83%), and edema (Grade 2-3) was present in four out of the six animals. These differences in epidermal erosion and presence of edema were not significant. The wounds were re-epithelialized with regenerated skin appendages in Group C, while the control group exhibited less re-epithelialization and regeneration of skin appendages (Figure 6(e), 6(f)).

MT staining revealed more organized collagen fiber deposition throughout the full thickness of the dermis layer when PDGF was administered (either alone or in combination with rMSCs) compared with the vehicle control (Figure 6(c), 6(d)).

To track the transplanted rMSCs, Dil-labeled rMSCs were traced at three and seven days postinjection. Dil-labeled rMSCs were observed at each time point and were located mainly between the epithelial layer and the dermis layer. Expression of PCNA was verified (Figure 7).

PART II. EFFECT ON RADIATION INDUCED BONY NECROSIS

A. Materials and methods

1. Materials

Hyaluronic acid (HA: MW 170,000 Da) was purchased from Lifecore Biomedical (Chaska, MN, USA) and 1-hyadroxybenzotriazole hydrate was purchased from Fluka Chemical (Buchs, Switzerland). 1-Ethyl-3-(3-dimethylaminopropyl)-

carbodimide, triethanolamine and adipic acid dihydrazide (ADH) were acquired from Sigma-Aldrich (St. Louis, MO, USA). N-acryloxysuccinimide was purchased from Acros Organics (Pittsburgh, PA, USA), and RGD peptides and MMP-insensitive peptides were obtained from AnyGen. (Gwang-ju, Korea). Escherichia coli-derived rhBMP-2 powder was provided from Daewoong Co. (Seoul, Korea), and dissolved with stabilizing buffer which was obtained by manufacture, at a concentration of 1 mg/mL. NFAT inhibitor (SigmaeAldrich, St. Louis, MO, USA) was prepared by dissolving 50% acetic acid at a concentration of 5 mM. Ficoll-paque plus was obtained from Amersham Biosciences (Uppsala, Sweden). Fetal bovine serum (FBS), penicillin/streptomycin, trypsin, and low-glucose Dulbecco's Modified Eagle's Medium (DMEM) were purchased from GIBCO BRL (Grand Island, NY, USA).

2. Preparation of hydrogel and synthesis of a MMP sensitive hyaluronic acid based hydrogel

Synthesis of MMP sensitive HA-based hydrogel was performed as described previously (39, 40). For gel preparation, MMP-sensitive peptides (GCRDGPQGIWGQDRCG) or MMP-insensitive peptides

(GCRDGDQGIAGFDRCG) were added to acrylated HA solution with the same molar ratio of acryl and thiol groups (41, 42). The HA-based hydrogel was formed using a Michael-type addition reaction (43). Cell adhesion peptides (RGDSP) were also immobilized on the acrylated HAs with a molar ratio of 20% of acryl groups of the HA. The reaction mixture was incubated at 37℃ for gelation. For each rat, 12 ㎕ of hydrogel (0.464 mg / 8 ㎕ of 4 wt % hydrogel with 230 kDa HA + 0.128 mg / 2 ㎕ of MMP sensitive peptides (80%) + 0.048 mg / 2㎕ RGD (20%)) were used. The mechanical properties and specific degradability of MMP sensitive HA-based hydrogels were described previously (39).

3. Preparation and culture of rat mesenchymal stem cells (rMSCs)

Bone marrow aspirate was obtained from rat tibias. MSCs were cultured as described previously in part I (36).

The hydrogels with or without 2 ㎕ of BMP-2 (10 ㎍/construct) were mixed with 2 ㎕ of PBS with passage 5 MSC suspensions (2 x 10^4 cells/construct) to produce a final volume of 16 ㎕ for each group. The samples were cross-linked for one hour at 37 ℃. The cells in the hydrogels were cultured in DMEM with 10% (v/v) FBS and 1%

(v/v) antibiotics, containing penicillin and streptomycin in a humidified incubator (5% CO_2, 37℃) overnight. MSC viability was verified in a previous experiment (41). The amount of rMSCs was determined by mixing a hydrogel construct with four different cell numbers (1×10^6 cells/construct, 1×10^5 cells/construct, 1×10^4 cells/construct, 2×10^4 cells/construct); the maximum cell number of rMSCs allowing for gelation was 2×10^4 cells/construct, and this amount was used for the experiment.

4. Animals and irradiation

One hundred fourteen Sprague-Dawley (SD) rats (seven-week-old male) (Orientbio Inc. Seongnam, Korea; average mass of 205 grams) were used. 49 rats died during the development of the ORN model (supplementary results), and 65 rats were included in this study. Six rats underwent only the surgery without irradiation as the negative control group. The negative control group was used in the development of the ORN model and to analyze the effects of hydrogel containing rMSCs or BMP-2. 59 rats received surgery after irradiation. Of these, nine rats were used for pilot experiments, in which three rats were utilized to confirm the occurrence of ORN four

weeks after surgery (Figure 8) and six rats were sacrificed to determine the appropriate dose of BMP-2. Hydrogels containing 5 ㎍, 10 ㎍, and 20 ㎍ of BMP-2 were administered to two rats for each dose, and the new bone formation was assessed after four weeks. The bone volume in the region of interest was 0.32 ㎣ in rats treated with 5 ㎍ BMP-2, 1.03 ㎣ in rats treated with 10 ㎍ BMP-2, and 0.37 ㎣ in rats treated with 20 ㎍ BMP-2. Therefore, we used 10㎍ of BMP-2 in this study. Finally, 50 rats which received irradiation were included to evaluate efficacy.

Before extraction, animals were irradiated using an X-ray (Clinac iX, Varian Medical System, Inc., Palo Alto, CA, USA). Under general anesthesia with Zoletil 50 (0.1mg/100g) (Virbac, Paris, France), the right mandible was shaved and disinfected with povidone-iodine solution (MEDICA KOREA, Seoul, Korea), and a single dose of 30 Gy (6 MeV electron, 600MU/min) was administered to the right mandibular body. Rats were housed individually to prevent gnawing of wounds and other potentially damaging interactions. One week after irradiation, three right mandibular molars were extracted and a bony defect was created under general anesthesia using intraperitoneal injection of ketamine hydrochloride (Ketara®, Yuhan Corp. Korea, 40

mg/kg) mixed with xylazine (Rumpen® Bayer Korea Ltd., Korea, 10 mg/kg). After molar extractions, a bone defect sized 4 ㎜ in length, 2 ㎜ in width, and 1.5 ㎜ in height was created with a surgical curette and a dental rotary handpiece.

The animals that underwent surgery after irradiation (n = 50) were divided into two groups (Table 3). In Group 1, the hydrogel construct was applied immediately after the extraction and creation of the bony defect (Groups 1b, 1c, 1d, 1e, n = 20), while the hydrogel construct was not inserted in the positive control (Group 1a, n = 5). In Group 2, the hydrogel construct was applied four weeks after surgery when ORN had already occurred (Groups 2b, 2c, 2d, 2e, n = 20), while the hydrogel construct was not inserted in the positive control (Group 2a, n = 5). In Group 1, the hydrogel construct was applied after verifying hemostasis, and wound closure was performed with 6-0 nylon. The maintenance of wound closure with the suture material was checked one, three, and seven days after surgery. In Group 2, we confirmed wound dehiscence in the exposed alveolar bone four weeks after surgery, and then the contaminated necrotic bone was removed by surgical curettage after wound disinfection. Thereafter, the hydrogel construct was applied and the primary wound closure was performed

with 6-0 nylon. As in Group 1, the maintenance of wound closure with the suture material was checked one, three, and seven days after surgery (Figure 8).

The sub-classifications of Group 1 and 2 are as follows, depending on the contents of hydrogel construct: Group 1a/2a (n=5 for each), no hydrogel in the bone defect; Group 1b/2b (n=5 for each), hydrogel (16 ㎕) only; Group 1c/2c (n=5 for each), hydrogel (16 ㎕) containing rMSCs (2 x 10^4 cells); Group 1d/2d (n=5 for each), hydrogel (16 ㎕) containing BMP-2 (10 ㎍); and Group 1e, 2e (n=5 for each), hydrogel (16 ㎕) containing rMSCs (2 x 10^4 cells) and BMP-2 (10 ㎍).

The occurrence of ORN was investigated during the harvest of the mandibular bone segment, whether alveolar bone was exposed or covered fully with soft tissue mucosa.

5. Micro-CT analysis

Micro-computed tomography was done with SkyScan 1172® (SkyScan®, Kontich, Belgium). The SkyScan 1172® microfocus X-ray system was equipped with a microfocus X-ray tube with a focal spot

of 2 ㎛, producing a cone beam that was detected by a 12-bit cooled X-ray camera that was charge coupled device (CCD) fiber-optically coupled to a scintillator. The resulting images for two-dimensional and three-dimensional (3D) analysis were square 512 x 512 pixel images. An optimized 3D cone beam reconstruction algorithm with a cluster volumetric reconstruction (Feldkamp algorithm) was used. The scan parameters were 20-100 kV, 10 W with rotation. A full three-dimensional image containing the experimental area and the surrounding trabecular bone was obtained with a cubic voxel size of 24 ㎛, resulting in about 400 two-dimensional images per specimen. Image analysis was done with CTAn 1.8® (SkyScan®, Kontich, Belgium), and 3D reconstruction was done with NRecon 1.6.9.8® (SkyScan®, Kontich, Belgium). Using three-dimensionally reconstructed images, regions demonstrating consistent bony necrosis and bone formation were designated as the region of interest (ROI). Each ROI was defined as a volume of 50 pixels in width by130 pixels in height by 132 pixels in length. Micro-CT image analysis was done by assessing the volume and quality of bone. Tooth root rests within the ROI were excluded, and only bone tissue was assessed. Roots could be distinguished from bone with the naked eye in each

cross-section and were well separated from bone by the surrounding radiolucent space (periodontal ligament). The specific thresholds for mineralized bone were defined by superimposing original segmented images over grayscale images. Equivalent thresholds were applied for every image to divide mineralized bone from the background. Within the ROI, bone mineral density (BMD) (%), bone volume (BV) (㎣), trabecular thickness (Tb.Th) (㎜), trabecular number (Tb.N) (1/㎜), and trabecular separation (Tb.Sp) (㎜) were measured and compared (Figure 9).

6. Histological evaluation

After Micro-CT reconstruction, we resected and decalcified the surgical fields at the mandible using ethylene diamine tetra-acetic acid solution (7%, pH 7.2) for 3-4 days, with replacement of the acid solution on day 2. The specimens were then dehydrated in 70% ethanol, fixed in 10% formalin-buffered solution (Duksan Pure Chemicals Co. Ansan-si, Korea), and embedded in paraffin wax (Leica Biosystems Nussloch GmbH, Nußloch, Germany). For histological staining, decalcified paraffin sections were cleaned with xylene

(Duksan Pure Chemicals Co.) for ten minutes, and four-㎛-thick slices were prepared and then stained with both hematoxylin and eosine Y (H&E) (Sigma-Aldrich) and Masson's trichrome (MT) (Sigma-Aldrich) to detect cells and regenerated bone structures. Digital images of the stained sections were collected for histological evaluation using a transmission and polarized light Axioskop microscope, Olympus BX51 (Olympus Corp., Tokyo, Japan). Bone tissue characteristics of the experimental and control groups were compared. Histomorphometric evaluation was not performed, because histological images did not represent osseous healing due to irregular healing patterns in the bony defects.

7. Statistical analysis

All data from computed tomographic scans were presented as mean ± standard error of mean in each experimental group (n = 5). The normality of the distribution of the data was confirmed qualitatively using the Kolmogorov-Smirnov test. Two-way ANOVA with a Bonferroni correction was used to analyze the effects of application time and application material. One way ANOVA was used to analyze the effect of the application material within groups. For the groups that

showed an abnormal distribution, the Kruskal–Wallis test was applied to compare the computed tomographic data. Results were considered statistically significant at $p < 0.05$. Statistical analysis was performed using SPSS 21.0 software (SPSS INC., Chicago, IL, USA).

B. Results

1. Development of the ORN Model in SD rats

The total number of animals in the beginning of the study (n = 114) was much greater than the number of animals included for the evaluation of efficacy (n = 65) when creating this rat ORN model. Molar roots were frequently fractured during extraction, and the alveolar bone exposure in extraction sockets differed depending on the existence and size of root rests. Therefore, a bone defect after molar extraction was created with a surgical curette and a dental rotary machine to create similar alveolar bone exposure in all animals. However, the creation of an alveolar bone defect in the rat mandible seemed too traumatic for the inferior alveolar artery, which often ruptured during this surgical procedure; 16 rats (14 rats in group 1, 2

rats in group 2) died due to excessive hemorrhage from the inferior alveolar artery or airway obstruction from a blood clot. Moreover, the pain resulting from damage to the inferior alveolar nerve during the surgical procedure woke animals up from the anesthesia, and the additional anesthetic injections led to complications (mainly overdose) in 15 rats (13 rats in group 1, 2 rats in group 2). 18 rats (10 rats in group 1, 8 rats in group 2) died during the postoperative check-up period with unclear etiology. Ultimately, only 65 rats were included in this experiment. The mortality for the development of ORN model was 43.0% (49/114 rats). The occurrence of bone necrosis without the coverage of mucosal soft tissue could be observed in all animals during the harvest of the mandibular bone segment for histological evaluation.

In Group 1, the postoperative follow-up period was four weeks. In Group 2, it was eight weeks because of the different administration time. Alopecia and undergrowth of the ipsilateral incisor were observed on the irradiated right side of the mandible. Hair loss and incisor undergrowth were not observed on the opposite side.

In the negative control group in the pilot experiment, where extraction was done without irradiation, 3D micro-CT analysis showed an average bone volume of 4.78 ± 1.53 ㎣ and an average

BMD of 1.50 ± 0.07% in the extraction socket four weeks after extraction. The experimental group in the pilot experiment showed an average bone volume of 2.26 ± 1.94 ㎣ and an average BMD of 1.34 ± 0.10%. Both bone volume and BMD were significantly lower in the experimental group from the pilot experiment (p=0.016, p=0.039, respectively). Histologically, bone loss and ingrowth of fibrotic tissue in the bone marrow of the irradiated area were observed. Blood vessels at the irradiated area were obstructed with signs of vitreous degeneration (Figure 10).

2. Effect of hydrogel with BMP-2 and MSCs depending on different application time.

2.1. Micro-CT results

2.1.1. Bone healing in Group 1

The mean values for BV and BMD are presented in Table 4. Among the subgroups in Group 1, only the positive control (Group 1a) showed clearly lower BV compared to the negative control; the BV of all other subgroups was similar or higher. BMD in Group 1c was similar to the negative control, while Group 1d had a higher BMD than the negative

control. BMD in other subgroups was lower than that of the negative control. Only Group 1d had more effective bone healing than the positive control; when BMP-2 was applied immediately after defect formation, BV and BMD were significantly higher four weeks after surgery than BV ($p = 0.001$) and BMD ($p = 0.002$) in the positive control (Group 1a) (Figure 11(a)). Application of rMSCs, either alone or in combination with BMP-2, had no significant effect on the increase in BV or BMD. Our results suggest that BMP-2 is effective for increasing both BV and BMD, while rMSCs are not effective for increasing BV and BMD (Figure 12). In addition, only BMP-2 alone effectively increased Tb. N compared to Group 1a (p=0.027). No significant differences among groups were found for Tb.Th and Tb.Sp.

2.1.2. Bone healing in Group 2

The mean BV and BMD values are presented in Table 4. Groups 2a and 2b showed clearly lower BV than the negative control, while Groups 2c, 2d and 2e had higher BV than the negative control. BMD in Groups 2c and 2e was similar to the negative control, while BMD was slightly lower in Group 2d and was clearly lower in Groups 2a/2b. Groups 2c, 2d and 2e had more effective healing than the positive

control (group 2a), indicating that BMP-2 and/or rMSCs application led to increased BV (Figure 11(b)). Group 2e showed a significant increase in BMD when compared to Group 2a (p=0.01) and Group 2b (p=0.000). Group 2c showed significantly increased BMD compared to Group 2b (p=0.002). These results suggested that application of rMSCs could increase BMD (Figure 13). Tb.Th was significantly increased in Groups 2c and 2d when compared to group 2b (p=0.006, p=0.008), and Tb.N was significantly increased in Group 2e when compared to group 2b (p=0.013). Tb.Sp showed no significant differences among groups.

2.2. Histological results

2.2.1. Development of ORN

Four weeks after extraction and bony defect formation in irradiated bone, specimens showed fibrosis, infiltration of inflammatory cells into inter-trabecular spaces, necrotic bony change of the trabecular bone, and empty lacunae (Figure 10).

2.2.2. Effect of hydrogel containing rMSCs or BMP-2 on jaw ORN

in rats

Epithelial tissue at the defect area was incompletely regenerated in Groups 1a and 1b, while Groups 1c, 1d, and 1e showed complete regeneration. In Groups 1c, 1d and 1e, normal bone/marrow structure could be observed, but there was slight inflammation in Groups 1a and 1b (Table 5) (Figure 14(a), 15(a), 15(b)).

In Group 2, epithelial tissue at the ORN area was poorly regenerated in Groups 1a and 2b, while Groups 2c, 2d, and 2e showed epithelial coverage of alveolar bone. In groups 2a and 2b, there was almost no new bone formation and no epithelial lining over the alveolar bone. In addition, we observed resorptive changes including inflammation and numerous empty lacunae. In contrast, when rMSCs were applied, there was almost no infiltration of inflammatory cells, and alveolar bone was regenerated with normal bone structure, but with small bone defects at the alveolar crest (Table 5) (Figure 14(b), 15(c), 15(d)).

2.1.3. Comparison between Group 1 and 2

BV was significantly smaller when hydrogel alone was applied after the occurrence of ORN (Group 2b) (1.32 ± 0.78 ㎣) when compared

to the rats who received an immediate application of hydrogel (Group 1b: 4.27 ± 0.45 ㎟) (p=0.034). Tb.N varied based on the time of BMP-2 application. BMP-2 application immediately after extraction resulted in significantly higher Tb.N (1.33 ± 0.44 /mm) compared to BMP-2 application after the occurrence of ORN (0.49 ± 0.11 /mm) (p=0.009). Otherwise, no significant differences were found between Groups 1 and 2.

DISCUSSION

In patients exposed to radiation therapy, radiation-induced skin irritations can cause undesired complications, such as soft tissue ulcers with reduced wound healing ability and prolonged healing progress. Additional alveolar bone trauma and surgery such as tooth extraction after irradiation to impaired soft tissue healing state are considered major initiating risk factors for ORN (6). Early treatment of radiation-induced tissue can lessen pain and reduce secondary infection and damage of adjacent tissues. Impaired wound healing in the oral mucosa and alveolar bone due to blood vessel damage after irradiation could be improved by exogenous or endogenous angiogenic factors (25). Recently, stem cell therapy has been proposed as a

complementary therapy to conventional surgical treatment for radiation-induced ulceration (12, 38, 44, 45). Bone marrow-derived MSCs can differentiate into myofibroblasts or epithelium can become blood vessel cells and perifollicular cells, which later form hair follicles during the wound healing process and play an important role in the formation of healthy tissues (46-48). Exogenous MSCs can produce growth factors for angiogenesis, such as VEGF and FGF (49, 50). Therefore, they can stimulate wound healing of hard and soft tissue lesions arising from local ischemia like ORN.

Although the precise mechanism by which bone marrow-derived mesenchymal stem cells aid wound healing is not yet clear, enhanced healing effects have been reported (51, 52). Several studies in irradiated animal models have reported therapeutic effects of allogenous or autologous human MSCs and rMSCs using a variety of application methods and times (12, 53-56). In the study by Huang et al., adipose-derived stem cells enhanced healing in irradiated skin lesions. Cells were injected three, four, and five weeks after irradiation and animals were sacrificed at three weeks after the first injection for soft tissue analysis. Part I of this study also demonstrated therapeutic effects on soft tissue immediately after injection; however,

extension of analysis to five weeks postinjection revealed no significant results. Histological examination showed that the epithelium tended to be less eroded in the rMSC treatment group compared with the control group. However, no significant differences were observed between the two groups. The different results regarding the effects of rMSCs may be due to factors such as the amount of radiation absorbed, the nature of the irradiation site, and the amount/origin of the MSCs.

In an analysis of the human and murine MSC transcriptomes, Tremain and colleagues found that MSCs express transcripts encoding proteins that regulate a broad range of biological activities, including angiogenesis and wound repair (22). Recent studies have suggested that the trophic capacity of MSCs to alter the tissue microenvironment may play a more prominent role than their transdifferentiation to achieve tissue repair (16, 23, 57, 58). This alteration to a more favorable tissue microenvironment may have led to the significantly increased bone volume in Group 2 of part II of the present study, where rMSCs were applied after the onset of ORN. In comparison, application of rMSCs immediately after bony defect formation was not as effective. Before the onset of ORN, the need for alteration in tissue

microenvironment would have been minimal.

Several efforts have been made to enhance the therapeutic effect of stem cells in the treatment of chronic wounds by administering them in combination with various growth factors (59, 60). PDGF has been reported to contribute to wound healing through its proangiogenic effects (61, 62). Moreover, PDGF is a major regulator of the growth, proliferation, survival, and chemotaxis of MSCs (63–65). Previous studies have reported that PDGF exerts therapeutic effects on wound healing (66–71). In this study, no significant difference was observed between the experimental and control sides when PDGF-BB was injected at the irradiated area (part I). Although similar doses of PDGF were used in the previous studies and in our study, the relative amount of PDGF was different in this study, since the previous studies used daily topical application while we performed subcutaneous injection. Also, the previous studies examined surgically formed wounds, while this study examined radiation-induced wounds. Improvement of wound healing by application of PDGF to radiation-damaged tissue was not observed in this study. Radiation exerts a negative effect on the mitogenic potential of PDGF (72); thus, the normal function of PDGF could have been impaired in irradiated skin.

Based on studies of interactions between MSCs and PDGF on the

cellular level (60, 73, 74), we investigated the clinical effect of applying MSCs in combination with PDGF. Yan et al. reported that human platelet-derived growth factor A-modified cultured cutaneous substitute cells (porcine bone marrow-derived mesenchymal stem cells and keratinocytes) promoted the healing of radiation-induced skin ulceration (73). After differentiation, MSCs primarily express PDGF receptor beta, which along with its ligand PDGF-β plays a key role in mediating tropism and differentiation during vascular remodeling (74). PDGF directly affecting differentiation and tropism of rMSCs during angiogenesis (75-78), a major process during skin regeneration, may have contributed to the significant therapeutic results seen in group c of this study where rMSCs and PDGF were applied in combination.

BMP-2, another prominent growth factor, has an angiogenic effect, in addition to stimulating osteogenesis (79). Implantation of recombinant human BMP-2/poly-lactide-co-glycolic acid in necrotic rabbit femoral heads helped recover from necrosis and increased the local blood supply to normal levels, with bone formation in the defective area after medullary cavity decompression (80). In addition, a gelatin sponge containing BMP-2 had angiogenic and osteogenic effects when it was applied to bony defects in the rabbit radius (81).

In the present study (part II), application of a hydrogel containing BMP-2 led to increased bone formation immediately after bony defect formation and after the onset of ORN. These results suggest that application of BMP-2 could be useful in treatment of ORN, where vessel formation capacity is decreased.

The healing effect of BMP-2 or rMSCs can differ depending on the time of application. Because the experimental conditions differ between groups 1 and 2, there is a limit in directly comparing the two groups. Within each group, differences in healing could be seen according to treatment modality. In this study (part II), the application of BMP-2 alone resulted in higher bone volume and bone mineral density than application of rMSCs alone when the hydrogel transplantation was done immediately after surgical trauma (Group 1). When the hydrogel transplantation was performed after ORN had occurred (Group 2), rMSC-applied specimens and BMP-2-applied specimens showed similarly enhanced bone volume; between the two, rMSC application brought about higher increase in BMD and Tb.Th. When BMP-2 and rMSCs were applied in combination, the most bone healing effect was seen by significant increases in BV, BMD, and Tb.N. The effect of rMSCs may have been more pronounced after the

occurrence of ORN due to the status of the recipient alveolar bone. Although animals in Group 2 received local debridement of the contaminated and necrotic recipient site, more contaminated residual necrotic alveolar bone and a lack of soft tissue coverage were also present in that group, where rMSCs could have played a role in the changing tissue microenvironment.

The 30-Gy single dose of radiation used in part II of the present study is higher than doses used in previous animal ORN models (82-86); however, bone necrosis did not occur in previous experiments. In 2011, Cohen et al. created a rat model of advanced ORN using high dose rate (30 Gy) brachytherapy (83) after molar extraction without an alveolar bone defect, where the mortality rate was 16% (1/6 rats). The mortality rate in the present study was much higher (43.0%). The main factors for this high mortality were complications during preparation of the surgical bone defect. These included severe bleeding from the inferior alveolar artery and vein after the removal of mandibular bone (14.0%) and anesthetic overdose (13.2%) to reduce pain after damage to inferior alveolar nerve, which is somewhat unavoidable when creating consistent bone defects. In order to objectively compare the osseous healing effects of BMP-2 and/or rMSCs among different groups, the initial osseous condition were kept

as constant as possible for each rat.

Hyaluronic acid based hydrogel is an excellent carrier for new bone formation. The bone forming effect of BMP-2 and/or human mesenchymal stem cell carried with hyaluronic acid hydrogel on rat calvarial defects was previously reported (41). Bae MS et al. reported the generation and effect of hyaluronic acid (HA) hydrogels loaded with growth and differentiation factor five on *in vitro* and *in vivo* osteogenesis (87). In particular, HA-based hydrogels synthesized using matrix metalloproteinase (MMP) sensitive acrylated HA mimicked the remodeling characteristics of natural extracellular matrices by cell-derived MMPs. These hydrogels have been reported to improve tissue remodeling rates and bone regeneration activity when used as scaffolds for BMP-2 and MSCs (40). In the present study, hydrogel was an effective carrier of BMP-2 and MSCs, as BV and BMD were increased or well-recovered in Groups 1d, 2c, 2d, and 2e.

This study demonstrated the therapeutic effects of growth factor and MSC application on necrotic soft and hard tissue following irradiation in rats. Further studies on middle and large sized animals are needed to investigate the application of MSCs and growth factors as treatment

modalities for radiation induced tissue necrosis.

CONCLUSION

In conclusion, neither rMSCs alone nor PDGF alone exerted any significant therapeutic effect in a rat model of radiation-induced soft tissue injury. However, when rMSCs were administered in combination with PDGF onto rat skin that already had radiation-induced soft tissue injury, the early stage of wound healing was significantly enhanced. Ulcer size also tended to be smaller when the rMSC/PDGF treatment was applied immediately after irradiation. These results will contribute to future efforts to successfully prevent and treat soft tissue ulceration that occurs as a complication of radiation therapy.

The present study also suggests that MSCs and/or BMP-2 carried with a hyaluronic acid-based hydrogel can be effective for bone regeneration in ORN. This effect may be enhanced immediately after dentoalveolar trauma or surgery by application of BMP-2. After the occurrence of ORN, the combined application of rMSCs and BMP-2

might be the most effective therapeutic approach.

REFERENCES

1. Marx RE. Osteoradionecrosis: a new concept of its pathophysiology. J Oral Maxillofac Surg. 1983;41(5):283-8.
2. Nabil S, Samman N. Risk factors for osteoradionecrosis after head and neck radiation: a systematic review. Oral surgery, oral medicine, oral pathology and oral radiology. 2012;113(1):54-69.
3. Wong JK, Wood RE, McLean M. Conservative management of osteoradionecrosis. Oral surgery, oral medicine, oral pathology, oral radiology, and endodontics. 1997;84(1):16-21.
4. Store G, Eribe ER, Olsen I. DNA-DNA hybridization demonstrates multiple bacteria in osteoradionecrosis. International journal of oral and maxillofacial surgery. 2005;34(2):193-6.
5. Delanian S, Lefaix JL. The radiation-induced fibroatrophic process: therapeutic perspective via the antioxidant pathway. Radiother Oncol. 2004;73(2):119-31.
6. Chrcanovic BR, Reher P, Sousa AA, Harris M. Osteoradionecrosis of the jaws--a current overview--part 1: Physiopathology and risk and predisposing factors. Oral and maxillofacial surgery. 2010;14(1):3-16.
7. Jagsi R, Ben-David MA, Moran JM, Marsh RB, Griffith KA, Hayman JA, et al. Unacceptable cosmesis in a protocol investigating intensity-modulated radiotherapy with active breathing control for accelerated partial-breast irradiation. Int J Radiat Oncol Biol Phys. 2010;76(1):71-8.
8. Hopewell JW. The skin: its structure and response to ionizing radiation. Int J Radiat Biol. 1990;57(4):751-73.
9. Rifkin LH, Stojadinovic S, Stewart CH, Song KH, Maxted MC, Bell MH, et al. An athymic rat model of cutaneous radiation injury designed to study human tissue-based wound therapy. Radiat Oncol. 2012;7:68.
10. Ilyin L. Radiation Medicine. Guide for Physicians and Researchers and Health Care Practitioners.: IzdAT; 2001.
11. O'Dell K, Sinha U. Osteoradionecrosis. Oral and maxillofacial surgery clinics of North America. 2011;23(3):455-64.

12. Kotenko K, Moroz B, Nadezhina N, Galstyan I, Eremin I, Deshevoy J, et al. Successful treatment of localised radiation lesions in rats and humans by mesenchymal stem cell transplantation. Radiat Prot Dosimetry. 2012;151(4):661-5.
13. Wang XJ, Lin S, Kang HF, Dai ZJ, Bai MH, Ma XL, et al. The effect of RHIZOMA COPTIDIS and COPTIS CHINENSIS aqueous extract on radiation-induced skin injury in a rat model. BMC Complement Altern Med. 2013;13:105.
14. Doctrow SR, Lopez A, Schock AM, Duncan NE, Jourdan MM, Olasz EB, et al. A synthetic superoxide dismutase/catalase mimetic EUK-207 mitigates radiation dermatitis and promotes wound healing in irradiated rat skin. J Invest Dermatol. 2013;133(4):1088-96.
15. Kitagawa J, Nasu M, Okumura H, Shibata A, Makino K, Terada H, et al. Allopurinol gel mitigates radiation-induced mucositis and dermatitis. J Radiat Res. 2008;49(1):49-54.
16. Iso Y, Spees JL, Serrano C, Bakondi B, Pochampally R, Song YH, et al. Multipotent human stromal cells improve cardiac function after myocardial infarction in mice without long-term engraftment. Biochem Biophys Res Commun. 2007;354(3):700-6.
17. Horwitz EM, Gordon PL, Koo WK, Marx JC, Neel MD, McNall RY, et al. Isolated allogeneic bone marrow-derived mesenchymal cells engraft and stimulate growth in children with osteogenesis imperfecta: Implications for cell therapy of bone. Proc Natl Acad Sci U S A. 2002;99(13):8932-7.
18. Oh SH CY, Kim BS, Yeo IB, Jo PK. The Effects of Undifferentiated Mesenchymal Stem Cells on Sinus Bone Grafting in Rabbit. J Korean Assoc Maxillofac Plast Reconstr Surg. 2006;28(6):520-30.
19. Ortiz LA, Dutreil M, Fattman C, Pandey AC, Torres G, Go K, et al. Interleukin 1 receptor antagonist mediates the antiinflammatory and antifibrotic effect of mesenchymal stem cells during lung injury. Proc Natl Acad Sci U S A. 2007;104(26):11002-7.
20. Kunter U, Rong S, Djuric Z, Boor P, Muller-Newen G, Yu D, et al. Transplanted mesenchymal stem cells accelerate glomerular healing in experimental glomerulonephritis. J Am Soc Nephrol. 2006;17(8):2202-12.
21. Minguell JJ, Erices A. Mesenchymal stem cells and the treatment of cardiac disease. Exp Biol Med (Maywood). 2006;231(1):39-49.

22. Tremain N, Korkko J, Ibberson D, Kopen GC, DiGirolamo C, Phinney DG. MicroSAGE analysis of 2,353 expressed genes in a single cell-derived colony of undifferentiated human mesenchymal stem cells reveals mRNAs of multiple cell lineages. Stem Cells. 2001;19(5):408-18.
23. Phinney DG, Prockop DJ. Concise review: mesenchymal stem/multipotent stromal cells: the state of transdifferentiation and modes of tissue repair--current views. Stem Cells. 2007;25(11):2896-902.
24. Singh S, Kloss FR, Brunauer R, Schimke M, Jamnig A, Greiderer-Kleinlercher B, et al. Mesenchymal stem cells show radioresistance in vivo. Journal of cellular and molecular medicine. 2012;16(4):877-87.
25. Springer IN, Niehoff P, Acil Y, Marget M, Lange A, Warnke PH, et al. BMP-2 and bFGF in an irradiated bone model. Journal of cranio-maxillo-facial surgery : official publication of the European Association for Cranio-Maxillo-Facial Surgery. 2008;36(4):210-7.
26. Xu J, Zheng Z, Fang D, Gao R, Liu Y, Fan Z, et al. Mesenchymal stromal cell-based treatment of jaw osteoradionecrosis in Swine. Cell transplantation. 2012;21(8):1679-86.
27. Quarto R, Mastrogiacomo M, Cancedda R, Kutepov SM, Mukhachev V, Lavroukov A, et al. Repair of large bone defects with the use of autologous bone marrow stromal cells. The New England journal of medicine. 2001;344(5):385-6.
28. Fouillard L, Bensidhoum M, Bories D, Bonte H, Lopez M, Moseley AM, et al. Engraftment of allogeneic mesenchymal stem cells in the bone marrow of a patient with severe idiopathic aplastic anemia improves stroma. Leukemia. 2003;17(2):474-6.
29. Bruder SP, Kurth AA, Shea M, Hayes WC, Jaiswal N, Kadiyala S. Bone regeneration by implantation of purified, culture-expanded human mesenchymal stem cells. Journal of orthopaedic research : official publication of the Orthopaedic Research Society. 1998;16(2):155-62.
30. Betsholtz C, Lindblom P, Gerhardt H. Role of pericytes in vascular morphogenesis. Exs. 2005(94):115-25.
31. Heldin CH, Westermark B. Mechanism of action and in vivo role of platelet-derived growth factor. Physiol Rev. 1999;79(4):1283-316.

32. Wurzler KK, DeWeese TL, Sebald W, Reddi AH. Radiation-induced impairment of bone healing can be overcome by recombinant human bone morphogenetic protein-2. The Journal of craniofacial surgery. 1998;9(2):131-7.
33. Osyczka AM, Diefenderfer DL, Bhargave G, Leboy PS. Different effects of BMP-2 on marrow stromal cells from human and rat bone. Cells, tissues, organs. 2004;176(1-3):109-19.
34. Chang SC, Chuang H, Chen YR, Yang LC, Chen JK, Mardini S, et al. Cranial repair using BMP-2 gene engineered bone marrow stromal cells. The Journal of surgical research. 2004;119(1):85-91.
35. Schultze-Mosgau S, Lehner B, Rodel F, Wehrhan F, Amann K, Kopp J, et al. Expression of bone morphogenic protein 2/4, transforming growth factor-beta1, and bone matrix protein expression in healing area between vascular tibia grafts and irradiated bone-experimental model of osteonecrosis. International journal of radiation oncology, biology, physics. 2005;61(4):1189-96.
36. Caterson EJ, Nesti LJ, Danielson KG, Tuan RS. Human marrow-derived mesenchymal progenitor cells: isolation, culture expansion, and analysis of differentiation. Molecular biotechnology. 2002;20(3):245-56.
37. Chung YL, Wang AJ, Yao LF. Antitumor histone deacetylase inhibitors suppress cutaneous radiation syndrome: Implications for increasing therapeutic gain in cancer radiotherapy. Mol Cancer Ther. 2004;3(3):317-25.
38. Lataillade JJ, Doucet C, Bey E, Carsin H, Huet C, Clairand I, et al. New approach to radiation burn treatment by dosimetry-guided surgery combined with autologous mesenchymal stem cell therapy. Regen Med. 2007;2(5):785-94.
39. Kim J, Park Y, Tae G, Lee KB, Hwang SJ, Kim IS, et al. Synthesis and characterization of matrix metalloprotease sensitive-low molecular weight hyaluronic acid based hydrogels. Journal of materials science Materials in medicine. 2008;19(11):3311-8.
40. Kim J, Kim IS, Cho TH, Kim HC, Yoon SJ, Choi J, et al. In vivo evaluation of MMP sensitive high-molecular weight HA-based hydrogels for bone tissue engineering. Journal of biomedical materials research Part A. 2010;95(3):673-81.
41. Kim J, Kim IS, Cho TH, Lee KB, Hwang SJ, Tae G, et al. Bone regeneration using hyaluronic acid-based hydrogel with bone morphogenic protein-2 and human mesenchymal stem cells. Biomaterials. 2007;28(10):1830-7.

42. Kim J, Park Y, Tae G, Lee KB, Hwang CM, Hwang SJ, et al. Characterization of low-molecular-weight hyaluronic acid-based hydrogel and differential stem cell responses in the hydrogel microenvironments. Journal of biomedical materials research Part A. 2009;88(4):967-75.
43. Hong SR, Chong MS, Lee SB, Lee YM, Song KW, Park MH, et al. Biocompatibility and biodegradation of cross-linked gelatin/hyaluronic acid sponge in rat subcutaneous tissue. Journal of biomaterials science Polymer edition. 2004;15(2):201-14.
44. Akita S, Akino K, Hirano A, Ohtsuru A, Yamashita S. Noncultured autologous adipose-derived stem cells therapy for chronic radiation injury. Stem cells international. 2010;2010:532704.
45. Kim J-Y, Kim M-R, Kim S-J. Modulation of osteoblastic/odontoblastic differentiation of adult mesenchymal stem cells through gene introduction: a brief review. Journal of the Korean Association of Oral and Maxillofacial Surgeons. 2013;39(2):55-62.
46. Yamaguchi Y, Kubo T, Murakami T, Takahashi M, Hakamata Y, Kobayashi E, et al. Bone marrow cells differentiate into wound myofibroblasts and accelerate the healing of wounds with exposed bones when combined with an occlusive dressing. Br J Dermatol. 2005;152(4):616-22.
47. Nakagawa H, Akita S, Fukui M, Fujii T, Akino K. Human mesenchymal stem cells successfully improve skin-substitute wound healing. Br J Dermatol. 2005;153(1):29-36.
48. Badiavas EV, Abedi M, Butmarc J, Falanga V, Quesenberry P. Participation of bone marrow derived cells in cutaneous wound healing. J Cell Physiol. 2003;196(2):245-50.
49. Zhang JC, Zheng GF, Wu L, Ou Yang LY, Li WX. Bone marrow mesenchymal stem cells overexpressing human basic fibroblast growth factor increase vasculogenesis in ischemic rats. Braz J Med Biol Res. 2014;47(10):886-94.
50. Bronckaers A, Hilkens P, Martens W, Gervois P, Ratajczak J, Struys T, et al. Mesenchymal stem/stromal cells as a pharmacological and therapeutic approach to accelerate angiogenesis. Pharmacol Ther. 2014;143(2):181-96.
51. Francois S, Mouiseddine M, Mathieu N, Semont A, Monti P, Dudoignon N, et al. Human mesenchymal stem cells favour healing of the cutaneous radiation syndrome in a xenogenic transplant model. Ann Hematol. 2007;86(1):1-8.

52. Deng W, Han Q, Liao L, Li C, Ge W, Zhao Z, et al. Engrafted bone marrow-derived flk-(1+) mesenchymal stem cells regenerate skin tissue. Tissue Eng. 2005;11(1-2):110-9.
53. Agay D, Scherthan H, Forcheron F, Grenier N, Herodin F, Meineke V, et al. Multipotent mesenchymal stem cell grafting to treat cutaneous radiation syndrome: development of a new minipig model. Exp Hematol. 2010;38(10):945-56.
54. Huang SP, Huang CH, Shyu JF, Lee HS, Chen SG, Chan JY, et al. Promotion of wound healing using adipose-derived stem cells in radiation ulcer of a rat model. J Biomed Sci. 2013;20(1):51.
55. Xia Z, Zhang C, Zeng Y, Wang T, Ai G. Transplantation of BMSCs expressing hVEGF(165) /hBD3 promotes wound healing in rats with combined radiation-wound injury. Int Wound J. 2012;11(3):293-303.
56. Koo M-A, Kang JK, Lee MH, Seo HJ, Kwon B-J, You KE, et al. Stimulated migration and penetration of vascular endothelial cells into poly (L-lactic acid) scaffolds under flow conditions. Biomater Res. 2014;18(2):48-54.
57. Gupta N, Su X, Popov B, Lee JW, Serikov V, Matthay MA. Intrapulmonary delivery of bone marrow-derived mesenchymal stem cells improves survival and attenuates endotoxin-induced acute lung injury in mice. J Immunol. 2007;179(3):1855-63.
58. Zhao Q, Gregory CA, Lee RH, Reger RL, Qin L, Hai B, et al. MSCs derived from iPSCs with a modified protocol are tumor-tropic but have much less potential to promote tumors than bone marrow MSCs. Proc Natl Acad Sci U S A. 2015;112(2):530-5.
59. Kawase Y, Yanagi Y, Takato T, Fujimoto M, Okochi H. Characterization of multipotent adult stem cells from the skin: transforming growth factor-beta (TGF-beta) facilitates cell growth. Exp Cell Res. 2004;295(1):194-203.
60. Hao L, Wang J, Zou Z, Yan G, Dong S, Deng J, et al. Transplantation of BMSCs expressing hPDGF-A/hBD2 promotes wound healing in rats with combined radiation-wound injury. Gene Ther. 2009;16(1):34-42.
61. Cipriani P, Di Benedetto P, Ruscitti P, Campese AF, Liakouli V, Carubbi F, et al. Impaired endothelium-mesenchymal stem cells cross-talk in systemic sclerosis: a link between vascular and fibrotic features. Arthritis Res Ther. 2014;16(5):442.
62. Ghosh D, Lili L, McGrail DJ, Matyunina LV, McDonald JF, Dawson MR. Integral role of platelet-derived growth factor in mediating transforming growth

factor-beta1-dependent mesenchymal stem cell stiffening. Stem Cells Dev. 2014;23(3):245-61.

63. Ponte AL, Marais E, Gallay N, Langonne A, Delorme B, Herault O, et al. The in vitro migration capacity of human bone marrow mesenchymal stem cells: comparison of chemokine and growth factor chemotactic activities. Stem Cells. 2007;25(7):1737-45.

64. Lienemann PS, Devaud YR, Reuten R, Simona BR, Karlsson M, Weber W, et al. Locally controlling mesenchymal stem cell morphogenesis by 3D PDGF-BB gradients towards the establishment of an in vitro perivascular niche. Integr Biol (Camb). 2014;7(1):101-11.

65. Sun X, Gao X, Zhou L, Sun L, Lu C. PDGF-BB-induced MT1-MMP expression regulates proliferation and invasion of mesenchymal stem cells in 3-dimensional collagen via MEK/ERK1/2 and PI3K/AKT signaling. Cell Signal. 2013;25(5):1279-87.

66. Brown RL, Breeden MP, Greenhalgh DG. PDGF and TGF-alpha act synergistically to improve wound healing in the genetically diabetic mouse. J Surg Res. 1994;56(6):562-70.

67. Chan RK, Liu PH, Pietramaggiori G, Ibrahim SI, Hechtman HB, Orgill DP. Effect of recombinant platelet-derived growth factor (Regranex) on wound closure in genetically diabetic mice. J Burn Care Res. 2006;27(2):202-5.

68. Park SA, Raghunathan VK, Shah NM, Teixeira L, Motta MJ, Covert J, et al. PDGF-BB does not accelerate healing in diabetic mice with splinted skin wounds. PLoS One. 2014;9(8):e104447.

69. Alexaki VI, Simantiraki D, Panayiotopoulou M, Rasouli O, Venihaki M, Castana O, et al. Adipose tissue-derived mesenchymal cells support skin reepithelialization through secretion of KGF-1 and PDGF-BB: comparison with dermal fibroblasts. Cell Transplant. 2012;21(11):2441-54.

70. Judith R, Nithya M, Rose C, Mandal AB. Application of a PDGF-containing novel gel for cutaneous wound healing. Life Sci. 2010;87(1-2):1-8.

71. Cohen MA, Eaglstein WH. Recombinant human platelet-derived growth factor gel speeds healing of acute full-thickness punch biopsy wounds. J Am Acad Dermatol. 2001;45(6):857-62.

72. Chung YL, Pui NN. Dynamics of wound healing signaling as a potential therapeutic target for radiation-induced tissue damage. Wound Repair Regen. 2015;23(2):278-86.

73. Yan G, Sun H, Wang F, Wang J, Wang F, Zou Z, et al. Topical application of hPDGF-A-modified porcine BMSC and keratinocytes loaded on acellular HAM promotes the healing of combined radiation-wound skin injury in minipigs. Int J Radiat Biol. 2011;87(6):591-600.
74. Betsholtz C. Insight into the physiological functions of PDGF through genetic studies in mice. Cytokine Growth Factor Rev. 2004;15(4):215-28.
75. Ball SG, Shuttleworth CA, Kielty CM. Mesenchymal stem cells and neovascularization: role of platelet-derived growth factor receptors. J Cell Mol Med. 2007;11(5):1012-30.
76. Phipps MC, Xu Y, Bellis SL. Delivery of platelet-derived growth factor as a chemotactic factor for mesenchymal stem cells by bone-mimetic electrospun scaffolds. PLoS One. 2012;7(7):e40831.
77. Hung BP, Hutton DL, Kozielski KL, Bishop CJ, Naved B, Green JJ, et al. Platelet-Derived Growth Factor BB Enhances Osteogenesis of Adipose-Derived But Not Bone Marrow-Derived Mesenchymal Stromal/Stem Cells. Stem Cells. 2015;Sep 33(9):2773-84.
78. Ng F, Boucher S, Koh S, Sastry KS, Chase L, Lakshmipathy U, et al. PDGF, TGF-beta, and FGF signaling is important for differentiation and growth of mesenchymal stem cells (MSCs): transcriptional profiling can identify markers and signaling pathways important in differentiation of MSCs into adipogenic, chondrogenic, and osteogenic lineages. Blood. 2008;112(2):295-307.
79. David L, Feige JJ, Bailly S. Emerging role of bone morphogenetic proteins in angiogenesis. Cytokine Growth Factor Rev. 2009;20(3):203-12.
80. Pan ZX, Zhang HX, Wang YX, Zhai LD, Du W. Effect of recombinant human bone morphogenetic protein 2/poly-lactide-co-glycolic acid (rhBMP-2/PLGA) with core decompression on repair of rabbit femoral head necrosis. Asian Pac J Trop Med. 2014;7(11):895-9.
81. Cao L, Wang J, Hou J, Xing W, Liu C. Vascularization and bone regeneration in a critical sized defect using 2-N,6-O-sulfated chitosan nanoparticles incorporating BMP-2. Biomaterials. 2014;35(2):684-98.
82. Niehoff P, Springer IN, Acil Y, Lange A, Marget M, Roldan JC, et al. HDR brachytherapy irradiation of the jaw - as a new experimental model of radiogenic bone damage. Journal of cranio-maxillo-facial surgery : official publication of the European Association for Cranio-Maxillo-Facial Surgery. 2008;36(4):203-9.

83. Cohen M, Nishimura I, Tamplen M, Hokugo A, Beumer J, Steinberg ML, et al. Animal model of radiogenic bone damage to study mandibular osteoradionecrosis. American journal of otolaryngology. 2011;32(4):291-300.
84. Koga DH, Salvajoli JV, Alves FA. Dental extractions and radiotherapy in head and neck oncology: review of the literature. Oral diseases. 2008;14(1):40-4.
85. Lorente CA, Song BZ, Donoff RB. Healing of bony defects in the irradiated and unirradiated rat mandible. Journal of oral and maxillofacial surgery : official journal of the American Association of Oral and Maxillofacial Surgeons. 1992;50(12):1305-9.
86. Kurihashi T, Iwata H, Nasu M, Yosue T. Experimental study on wound healing of alveolar bone sockets in the rat maxilla after X-ray irradiation. Odontology / the Society of the Nippon Dental University. 2002;90(1):35-42.
87. Bae MS, Ohe JY, Lee JB, Heo DN, Byun W, Bae H, et al. Photo-cured hyaluronic acid-based hydrogels containing growth and differentiation factor 5 (GDF-5) for bone tissue regeneration. Bone. 2014;59:189-98.

Table 1. Modified skin score

Modified Skin Score (Mean ± SD)		Days after administration										
		0	3	7	10	14	17	21	24	28	31	35
Group A	MSCs	3.17 ± 1.22	3.08 ± 0.20	3.08 ± 0.81	2.67 ± 0.26	2.58 ± 0.29	2.58 ± 0.20	2.58 ± 0.24	2.42 ± 0.20	2.42 ± 0.63	2.42 ± 0.20	2.33 ± 1.03
	control	3.17 ± 0.26	3.00 ± 0.00	2.92 ± 0.20	2.67 ± 0.26	2.67 ± 0.26	2.50 ± 0.00	2.50 ± 0.00	2.50 ± 0.00	2.50 ± 0.00	2.50 ± 0.00	2.50 ± 0.00
Group B	PDGF	3.25 ± 0.27	3.17 ± 0.26	3.00 ± 0.00	2.75 ± 0.27	2.67 ± 0.26	2.67 ± 0.26	2.67 ± 0.26	2.50 ± 0.00	2.50 ± 0.00	2.50 ± 0.00	2.33 ± 0.26
	control	3.17 ± 0.26	3.00 ± 0.00	2.92 ± 0.20	2.75 ± 0.27	2.67 ± 0.26	2.50 ± 0.32	2.50 ± 0.32	2.42 ± 0.20	2.42 ± 0.20	2.42 ± 0.20	2.17 ± 0.26
Group C	MSCs + PDGF	3.20 ± 0.27	2.90 ± 0.22	2.90 ± 0.27	2.80 ± 0.27	2.80 ± 0.27	2.80 ± 0.27	2.80 ± 0.27	2.60 ± 0.22	2.60 ± 0.22	2.60 ± 0.22	2.20 ± 0.27
	control	3.10 ± 0.22	3.00 ± 0.35	2.90 ± 0.22	2.70 ± 0.27	2.70 ± 0.27	2.70 ± 0.27	2.70 ± 0.27	2.60 ± 0.22	2.60 ± 0.22	2.50 ± 0.00	2.40 ± 0.22

Table 2. Ulceration in percentage

Ulceration in percentage (%) (Mean ± SD)		Days after administration										
		0	3	7	10	14	17	21	24	28	31	35
Group A	MSCs	46.81 ± 10.35	40.46 ± 9.98	29.26 ± 12.73	22.96 ± 14.47	19.47 ± 12.58	14.80 ± 15.36	12.05 ± 13.96	8.10 ± 9.92	6.44 ± 8.63	4.36 ± 6.30	0.57 ± 0.71
	control	45.19 ± 10.32	36.93 ± 12.54	24.01 ± 9.02	18.78 ± 8.19	18.89 ± 13.45	11.02 ± 6.49	7.17 ± 5.31	4.98 ± 4.11	3.31 ± 2.31	3.70 ± 2.89	0.92 ± 1.06
Group B	PDGF	50.22 ± 5.10	41.46 ± 7.70	28.42 ± 10.73	22.96 ± 14.20	19.48 ± 16.02	14.52 ± 13.83	10.84 ± 13.16	8.05 ± 11.08	5.90 ± 8.43	5.05 ± 7.02	2.09 ± 4.16
	control	45.11 ± 6.78	42.62 ± 5.28	27.76 ± 13.80	24.87 ± 13.82	23.43 ± 15.83	14.71 ± 14.08	10.69 ± 12.01	6.92 ± 8.20	4.76 ± 7.13	4.02 ± 7.42	2.80 ± 6.62
Group C	MSCs + PDGF	44.39 ± 7.54	31.56 ± 14.03*	25.00 ± 10.49*	18.58 ± 11.45**	18.20 ± 13.46	14.09 ± 13.00	12.56 ± 13.80	8.47 ± 10.11	6.30 ± 7.31	6.42 ± 7.22	1.15 ± 2.10
	control	46.39 ± 15.47	35.79 ± 14.07*	26.57 ± 11.18*	20.60 ± 10.42**	17.21 ± 10.86	13.22 ± 9.76	8.06 ± 9.16	6.05 ± 6.71	4.94 ± 5.21	3.29 ± 4.79	1.34 ± 1.34

Table 3. Classification of groups.

Group	Radiation	Time of defect formation after radiation	Time of hydrogel application after radiation	Treatment
Negative control	no radiation	0 week	0 weeks	Defect formation only
1a	radiation	1 week	1 week	Defect formation only
1b				Hydrogel application immediate after defect formation
1c				Hydrogel + rMSCs application immediate after defect formation
1d				Hydrogel + BMP−2 application immediate after defect formation
1e				Hydrogel + rMSCs + BMP−2 application immediate after defect formation
2a	radiation	1 week	5 weeks	Curettage only
2b				Hydrogel application immediate after curettage
2c				Hydrogel + rMSCs application immediate after curettage
2d				Hydrogel + BMP−2 application immediate after curettage
2e				Hydrogel + rMSCs + BMP−2 application immediate after curettage

Table 4. Data (average ± SD) of BV and BMD in each group.

		BV (㎣)	BMD (%)
Negative control(no radiation)		4.78 ± 1.53	1.50 ± 0.07
Group 1	Positive control	2.26 ± 1.94	1.34 ± 0.10
	Hydrogel	4.27 ± 0.45	1.40 ± 0.05
	Hydrogel + rMSCs	4.51 ± 0.45	1.48 ± 0.05
	Hydrogel + BMP-2	6.29 ± 1.63	1.58 ± 0.08
	Hydrogel + rMSCs + BMP-2	4.87 ± 1.29	1.44 ± 0.08
Group 2	Positive control	1.98 ± 0.71	1.32 ± 0.07
	Hydrogel	1.32 ± 0.79	1.26 ± 0.03
	Hydrogel + rMSCs	5.41 ± 1.77	1.48 ± 0.12
	Hydrogel + BMP-2	5.71 ± 0.94	1.44 ± 0.05
	Hydrogel + rMSCs + BMP-2	5.15 ± 1.55	1.53 ± 0.12

Table 5. Soft tissue coverage at the end of experiment.

Group	Soft tissue coverage (n)			Total (n)
	Non-covered	Partially covered	Completely covered	
Negative control			6	6
1a	1	4		5
1b	2	3		5
1c		1	4	5
1d		1	4	5
1e		2	3	5
2a	2	3		5
2b	2	3		5
2c		2	3	5
2d		1	4	5
2e			5	5

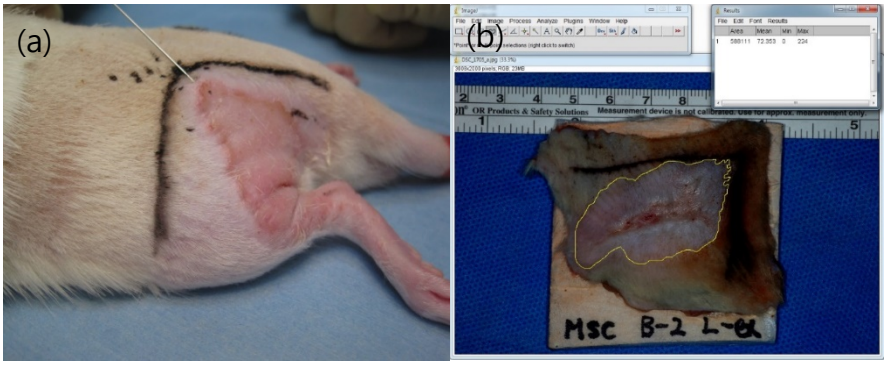

Figure 1. Analysis of ulcer size. (a) Image of a representative wound. B) Calculation of ulcer size using Image J.

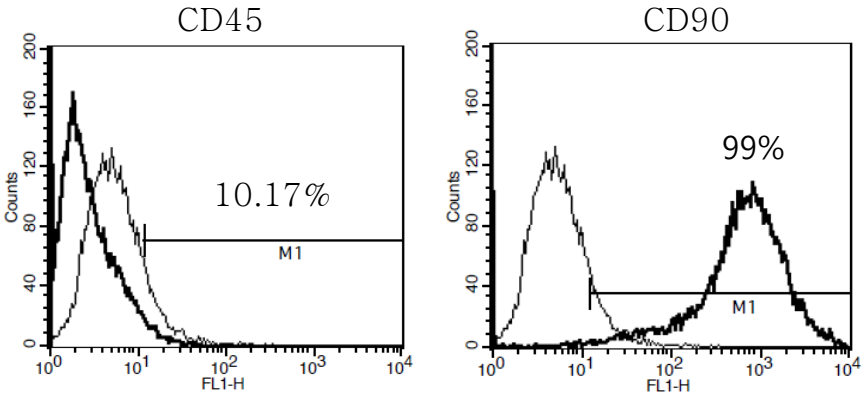

Figure 2. Flow cytometry. Flow cytometric analysis showing the expression of CD45 and CD90.

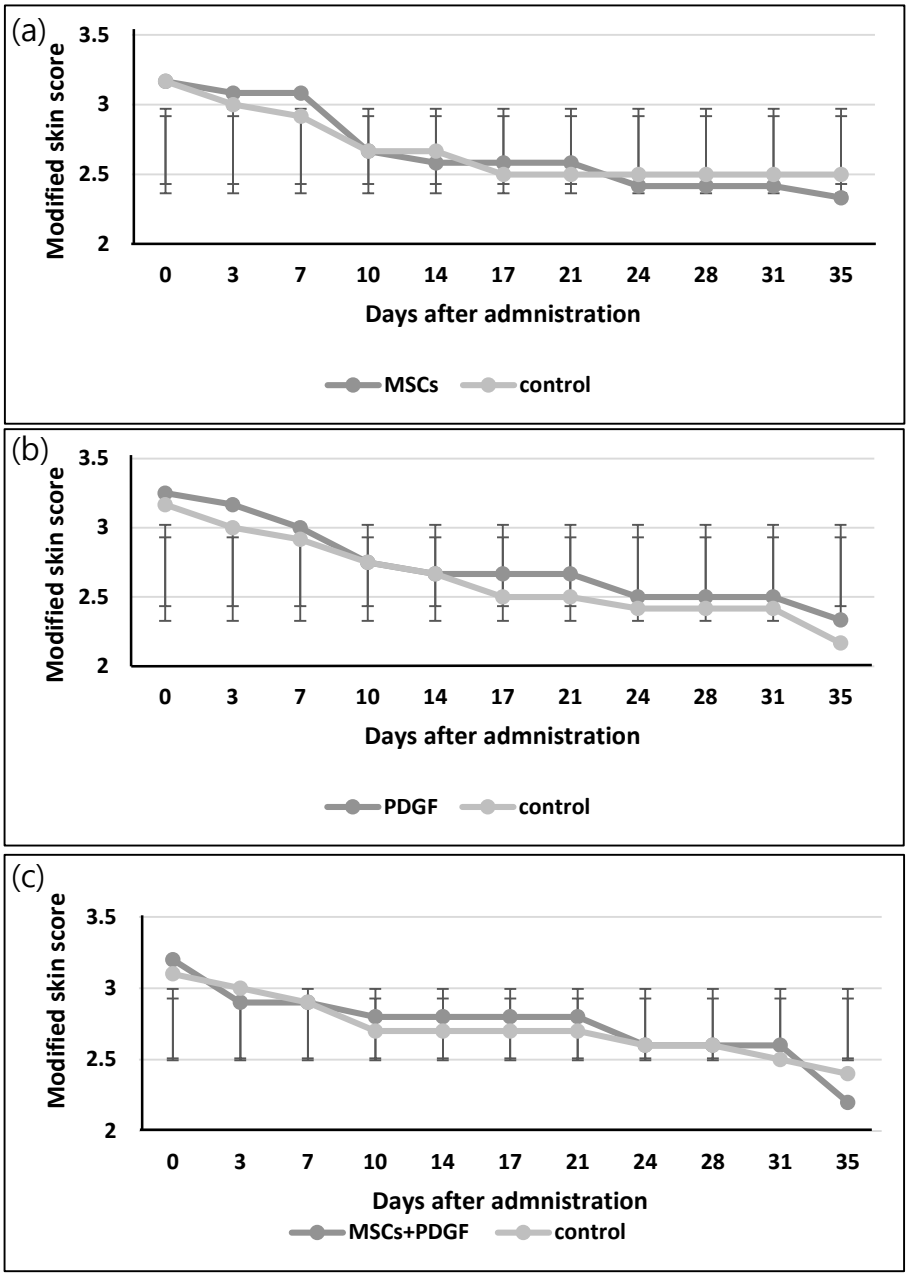

Figure 3. Modified skin scores. Changes in the modified skin scores after injection of (a) rMSCs (Group A), (b) PDGF (Group B), and (c) rMSCs + PDGF (Group C)

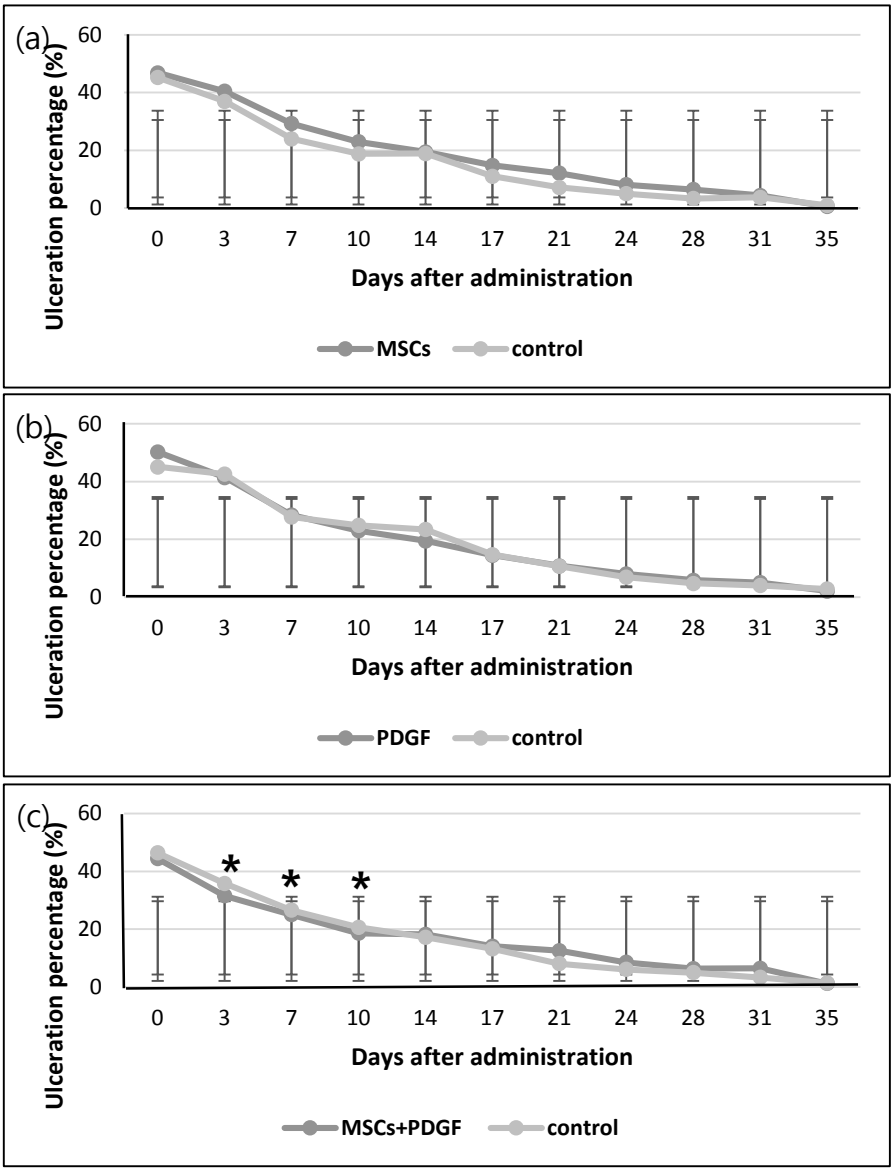

Figure 4. Skin ulceration ratio. Changes of the skin ulceration ratios (%) in (a) Group A (rMSCs), (b) Group B (PDGF), and (c) Group C (rMSCs + PDGF). Asterisks indicate statistically significant differences ($p \leq 0.05$).

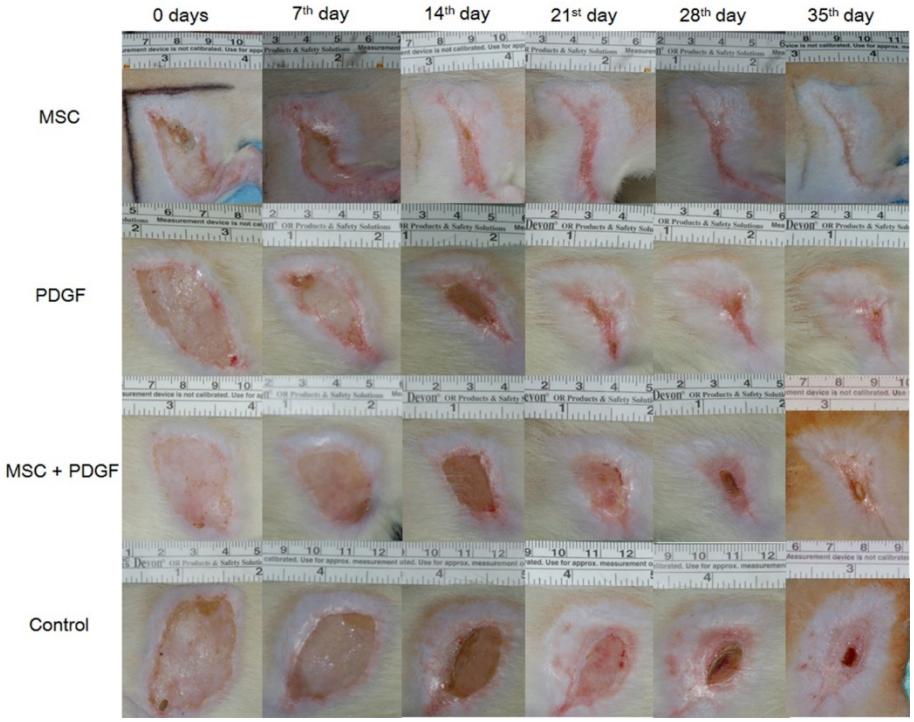

Figure 5. Photography of skin wound. Wound healing progress in Group A (rMSCs), B (PGDF), and C (rMSCs + PDGF) at different stages of healing.

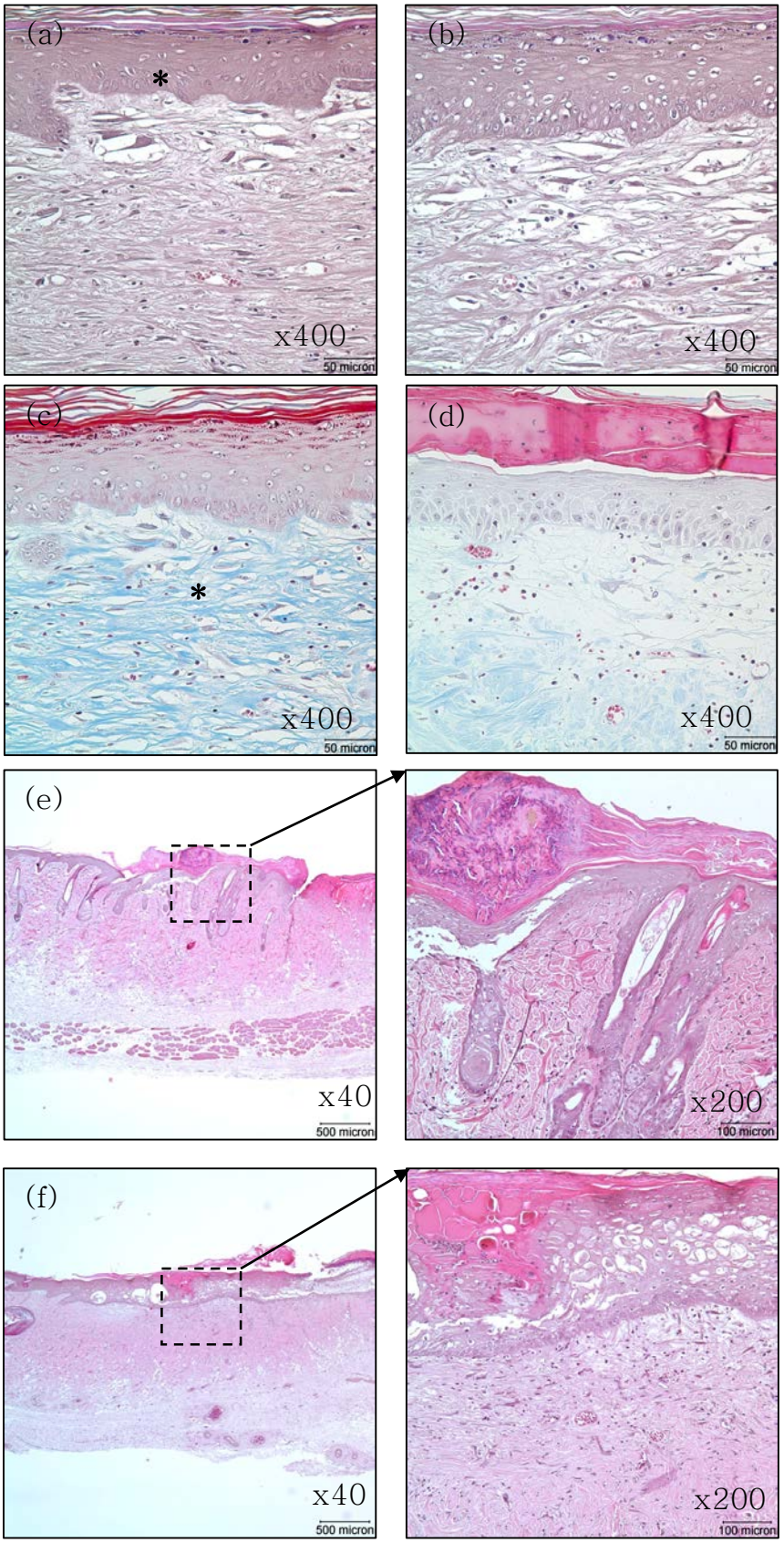
(a)
x400
50 micron
(b)
x400
50 micron
(c)
x400
50 micron
(d)
x400
50 micron
(e)
x40
500 micron
x200
100 micron
(f)
x40
500 micron
x200
100 micron

Figure 6. Histology. Histological images of radiation-induced skin wounds at 35 days postinjection. (a) HE staining of a representative skin wound from Group A (MSC treatment). Less edema (asterisk) was observed compared with the vehicle control (b). (c) Representative skin wound from Group B (PDGF treatment). More highly organized collagen fiber deposition (asterisk) was observed throughout the entire dermis layer compared with the vehicle control (d). (e) HE staining of a representative skin wound from Group C (rMSCs + PDGF). The wound was re-epithelialized with regenerated skin appendages (arrow). (f) HE staining of a representative skin wound from the control side in Group C. Reduced re-epithelialization and regeneration of skin appendages was observed compared with experimental side.

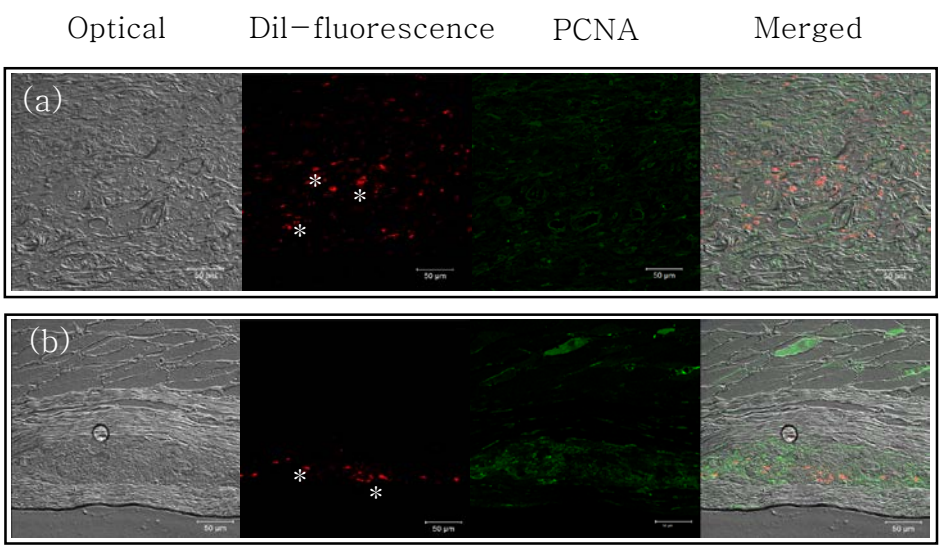

Figure 7. rMSCs tracking. Tracking of injected rMSCs at three (a) and seven (b) days after injection. Cultured rMSCs were labeled with fluorescent dialkylcarbocyanine (Dil) dye (10 ng/mL) and subcutaneously injected into the radiation-induced ulcer area at three weeks postirradiation. Proliferating cell nuclear antigen (PCNA) (green) was used to confirm the viability of the rMSCs. rMSCs appeared near the basal membrane. *Dil-labeled MSCs observed in vivo.

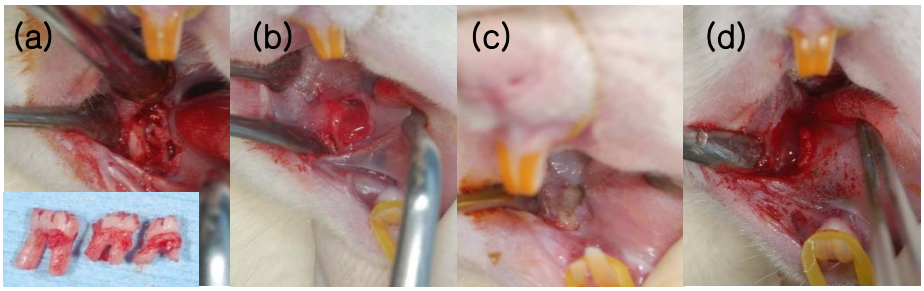

Figure 8. Surgery. (a) All three molars on the right side of the rat mandible were extracted, and afterwards the bony defect was formed. (b) In group 1, hydrogel was applied immediately. (c, d) In group 2, ORN was verified four weeks after formation of the bony defect, and a flap was elevated to perform curettage of contaminated denuded bone, after which the hydrogel was applied.

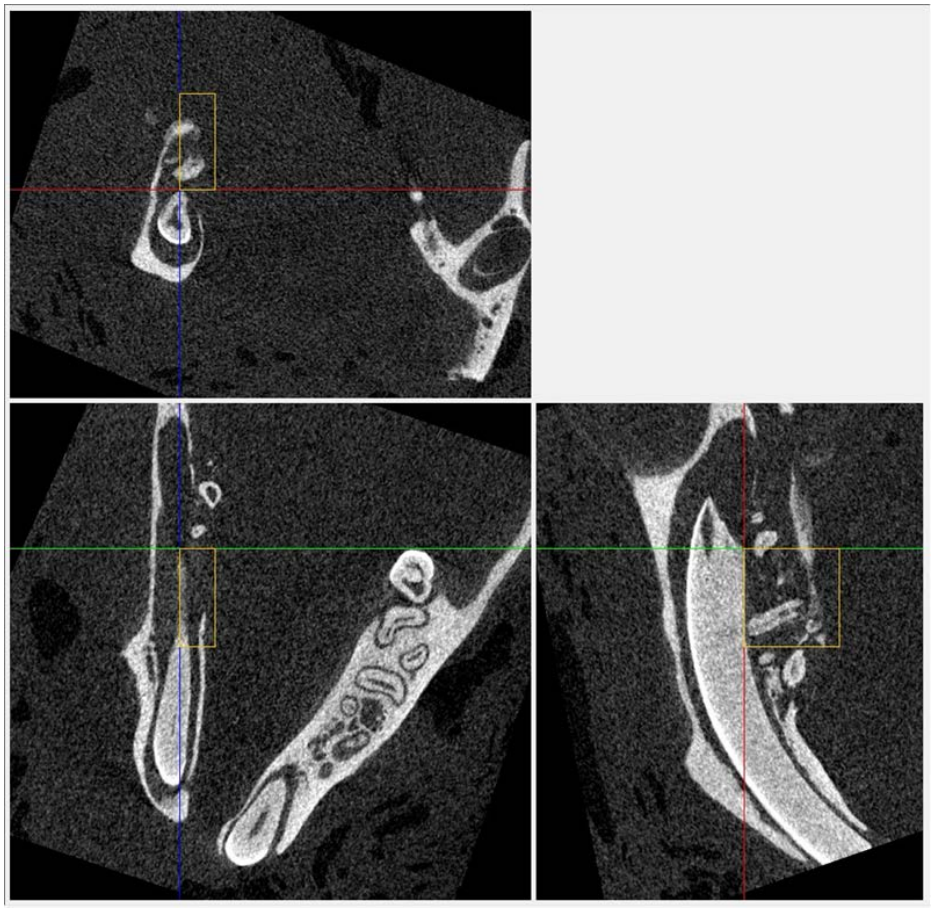

Figure 9. Definition of ROI. ROI was defined as a volume of width 50 height 130 and length 132 pixels.

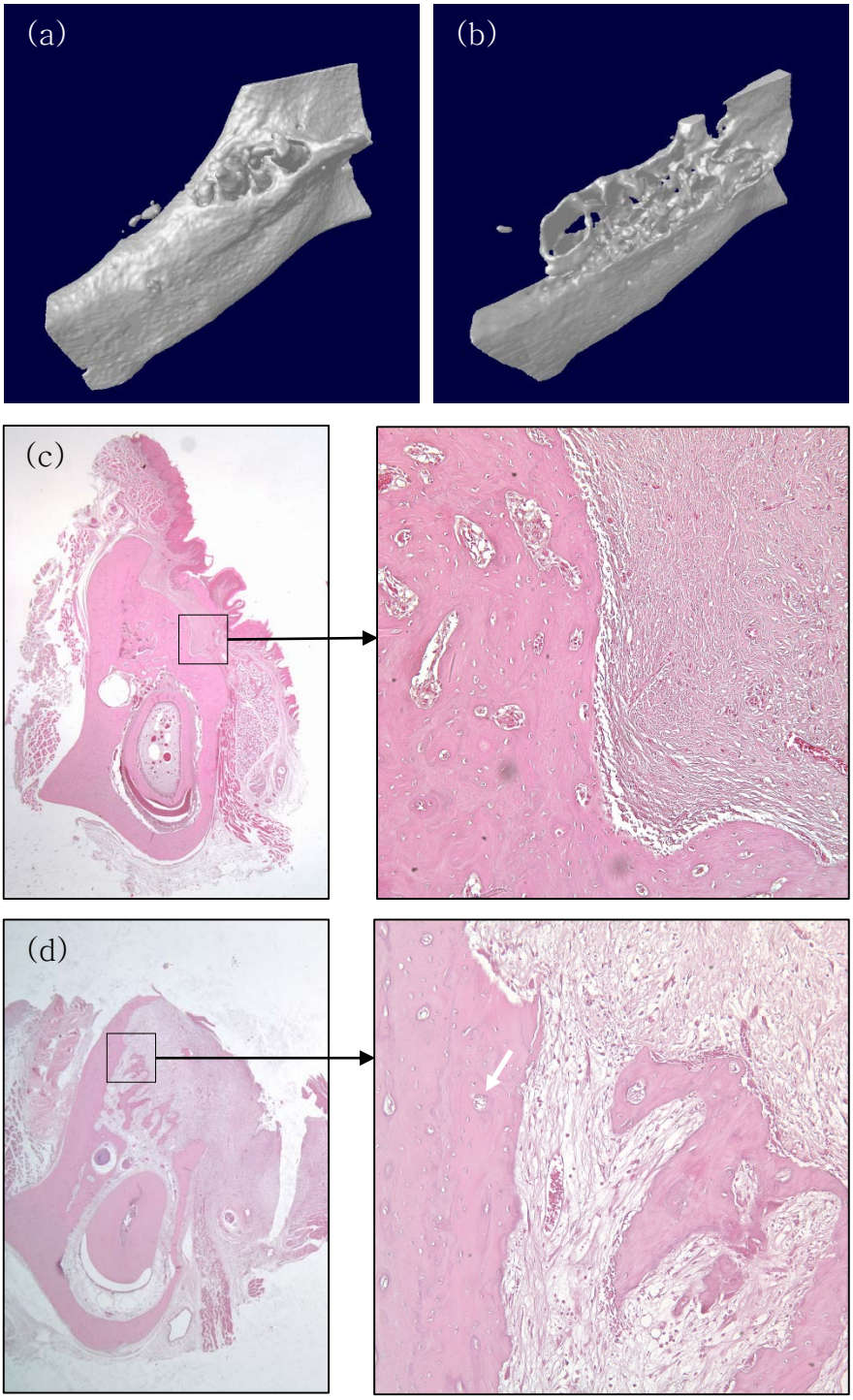
(a)
(b)
(c)
(d)

Figure 10. Occurrence of osteoradionecrosis. 3D micro-CT image and histological image (HE staining) four weeks after extraction of molars in the negative control (no radiation) and positive control (radiation only). (a) 3D micro-CT image of mandible with normal extraction socket in the negative control; (b) 3D micro-CT image of a mandible with ORN at the extraction socket in the positive control; (c) histological image of a mandible with a normal extraction socket in the negative control; (d) histological image of a mandible with ORN at the extraction socket in the positive control; exposed alveolar bone without epithelial coverage, obliterated blood vessels and reduced bone marrow space are shown (white arrow). 12.5x, 400x.

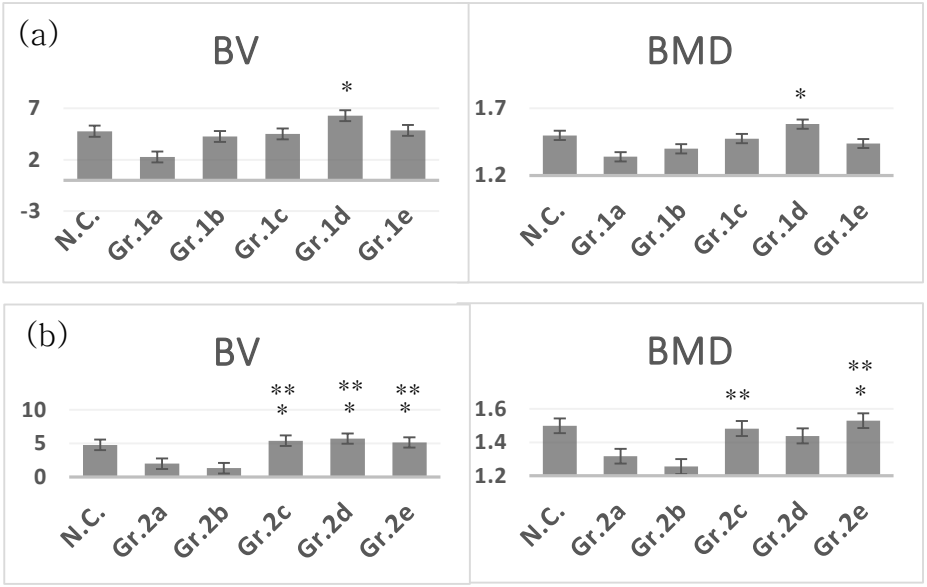

Figure 11. BV and BMD in Groups 1 (a) and 2 (b). (a) BV and BMD were significantly greater in Group 1d than in Group 1a. The asterisk (*) indicates a p−value of <0.05 (p=0.001 and p=0.002, respectively) compared to the positive control (Group 1a). N.C. indicates the negative control. Gr.1a: positive control in group 1; Gr.1b: hydrogel only; Gr.1c: hydrogel containing rMSCs; Gr.1d: hydrogel containing BMP−2; Gr.1e: hydrogel containing rMSCs and BMP−2. (b) Groups 2c, 2d and 2e had significantly greater BV than Group 2a. The asterisk (*) indicates a p−value of <0.05 (p=0.003, p=0.002 and p=0.015, respectively) compared to the positive control (Group 2a). Groups 2c,

2d and 2e had significantly greater BV than Group 2b. The asterisk (**) indicates a p-value of <0.05 (p=0.000, p=0.000 and p=0.001, respectively) compared to hydrogel only (Group 2b). BMD in Group 2e was significantly greater than Group 2a. The asterisk (*) indicates a p-value of <0.05 (p=0.01) BMD in Group 2c and 2e were significantly greater than Group 2b. The asterisk (**) indicates a p-value of <0.05 (p=0.002 and p=0.000, respectively) compared to hydrogel only (Group 2b). N.C. indicates negative control. Gr.2a: positive control in group 2; Gr.2b: hydrogel only; Gr.2c: hydrogel containing rMSCs; Gr.2d: hydrogel containing BMP-2; Gr.2e: hydrogel containing rMSCs and BMP-2.

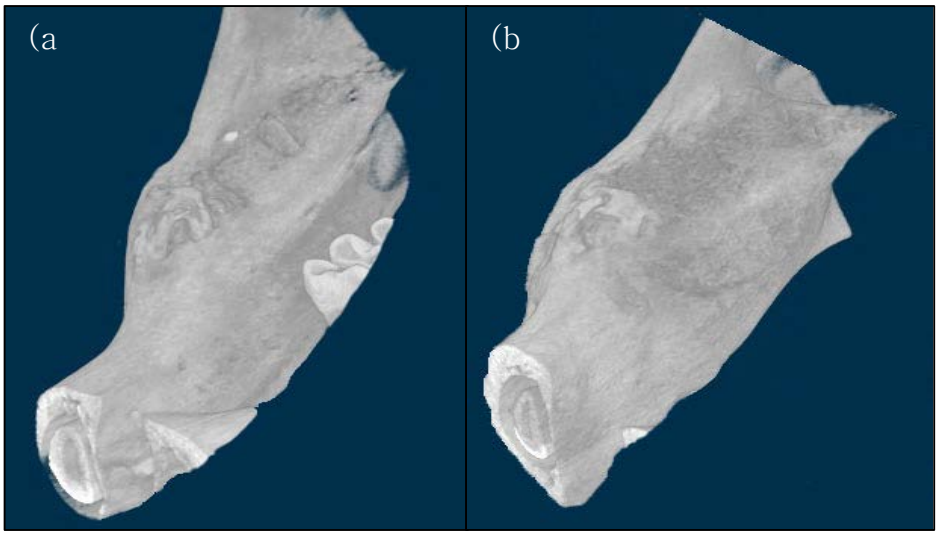

Figure 12. 3D reconstruction of micro CT images in Group 1. (a) Group 1a. Bone resorption is observed. (b) Group 1d. Following hydrogel application containing BMP-2, increase in BV was observed.

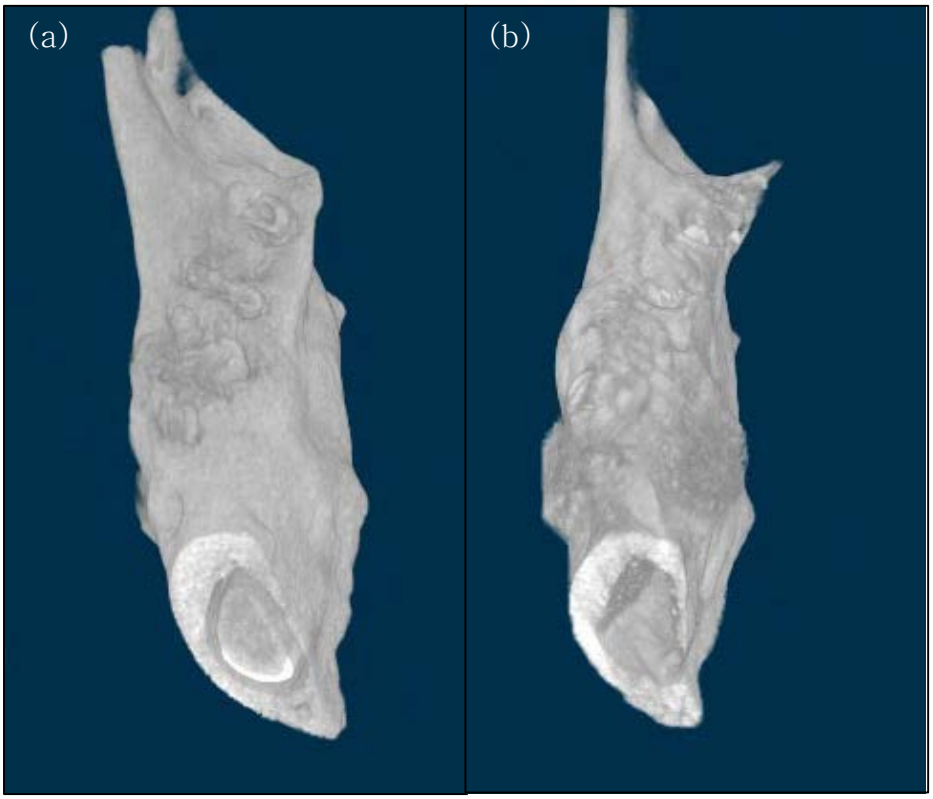

Figure 13. (a) Group 2a. Bone resorption is observed. (b) Group 2e. Following hydrogel application containing both rMSCs and BMP-2, increase in BV and BMD were observed.

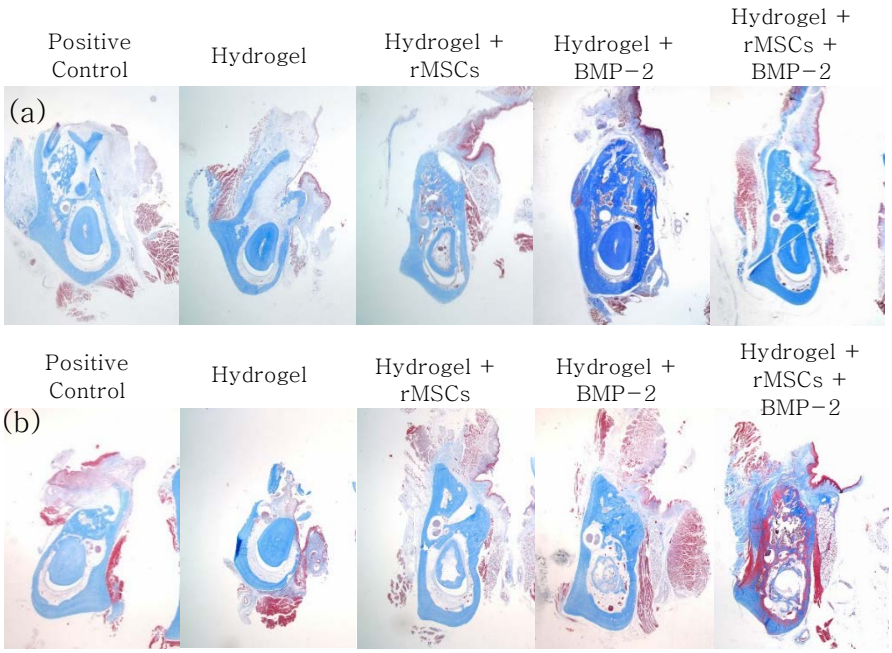

Figure 14. Histological evaluation of a mandibular defect model after a four−week application of hydrogel in Groups 1 and 2. (a) Incomplete regeneration of the epithelium with delayed bone healing in Groups 1a and 1b, but new bone formation with full coverage of the oral epithelium in Groups 1c, 1d, and 1e. (b) Incomplete regeneration of the epithelium with delayed bone healing was observed in Groups 2a and 2b, while new bone formation with full coverage of oral epithelium was observed in Groups 2c, 2d, and 2e. Masson Trichrome staining, 12.5x.

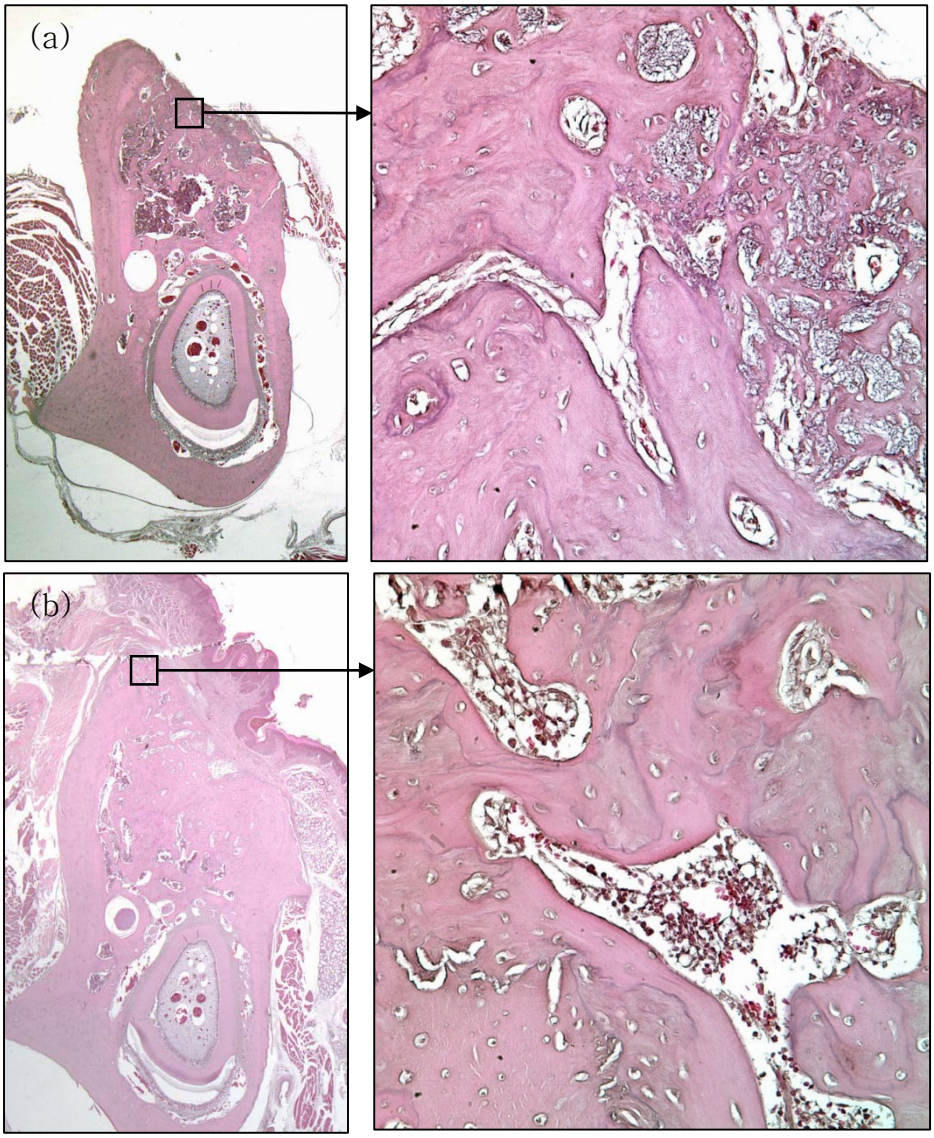
(a)
(b)

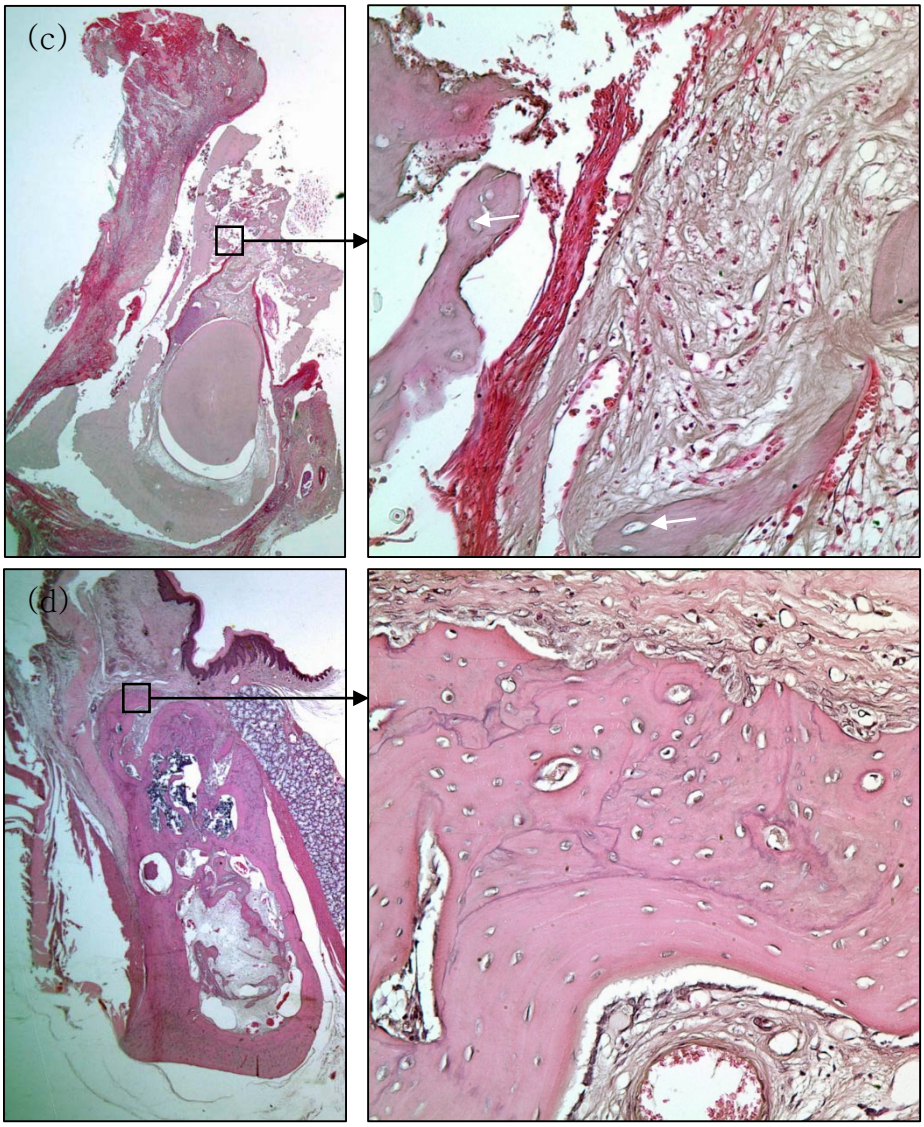

Figure 15. Comparison of histological results between Groups 1 and 2. (a) Regenerated alveolar bone with slight inflammation, even with incomplete epithelial regeneration in Group 1b; (b) normal bone structure without inflammation under full coverage of oral epithelial tissue in Group 1d; (c) no new bone formation and epithelial lining, in

addition to resorptive changes with inflammation in Group 2b; (d) regenerated alveolar bone with normal bone structure, but a small bone defect at the alveolar crest in Group 2e. H&E staining, 12.5x, 400x.

-국문초록-

백서에서 방사선조사에 의한 피부궤양과 골괴사 치료를 위한 골수유래 줄기세포와 PDGF/BMP-2의 적용 효과

진 임 건

서울대학교 대학원 치의과학과 구강악안면외과학 전공

(지도교수 황 순 정)

연구 목적

악골의 방사선골괴사(ORN)는 악안면 영역의 방사선 치료 이후 발생하는 주요 합병증 중 하나로 대증요법만으로 치유되는 경우도 있으나 경우에 따라 악골의 변형 및 악골기능의 손상을 유발하기도 하며 이 경우 결손부의 재건수술이 이루어지더라도 그 경과가 만족스럽지 못한 경우가 많다. 방사선골괴사는 방사선 조사 후 연조직 혹은 점막의 손상으로 골조직이 노출된 후 3~6개월간 치유되지 않고 지속되는 병변으로 정의된다. 방사선골괴사의 초기 단계에서는 연조직의 괴사가 발생하고 골조직의 노출이 일어나며 방사선골괴사가 진행됨에 따라 노출된 피질골 뿐만 아니라 하방의 망상골 또한 괴사되고 결국 괴사는 하악골의 하연까지 진행된다. 방사선골괴사의 기전은 명확하게 정립되어 있지 않아 방사선골괴사에 대한 직접적인 치료법은 확립되지 못했다. 방사선골괴사는 연조직의 괴사에서 시작되기 때문에 연조직 병변 단계에서 조직의 치유를 촉진하거나 괴

사의 진행을 늦출 수 있다면 이어지는 골조직의 노출을 최소화할 수 있다. 골조직의 노출 이후에는 골괴사 단계에서 골조직의 치유를 촉진할 수 있다면 방사선골괴사의 치료를 기대할 수 있다. 최근, 골수유래줄기세포의 상처치유에 대한 다양한 효과들이 보고된 바 있다. 그러나 방사선골괴사의 진행 단계에 있어서 골수유래줄기세포 단독으로 혹은 성장인자와 함께 적용하여 그 치유 효과에 대한 연구는 부족한 편이다. 이에 본 연구에서는 골수유래줄기세포 단독 혹은 혈소판유래 성장인자(platelet derived growth factor, PDGF)와 함께 적용하여 골수유래줄기세포 혹은 혈소판유래 성장인자가 백서에서의 방사선 유발 연조직 병변의 치유에 미치는 영향을 규명하고 백서 하악골의 방사선골괴사 모델에 골수유래줄기세포 단독 혹은 골형성단백질-2와 함께 적용하여 적용시기에 따른 골조직의 치유에 미치는 효과를 규명하고자 하였다.

Part I. 방사선 유발 연조직 손상부에 대한 효과

[재료 및 방법]

17마리의 백서(Sprague-Dawley) 좌우 둔부에 50 Gy의 방사선을 조사하였다. 방사선 조사 후 3주후 우측 둔부에는 대조군으로 인산염 완충용액을 적용하였고, 좌측 둔부는 골수유래줄기세포(rMSCs)(2×10^6 cells) 단독 적용, 혈소판유래 성장인자 (8 μg) 단독 적용 혹은 골수유래줄기세포 및 혈소판유래 성장인자 혼합 적용을 시행하였다. 상처치유는 적용 후 5주간의 치유 기간 동안 전체 방사선 조사부 대비 잔존 궤양 면적 비율

을 측정하여 분석하였고, 치유기간 동안 정량적 평가법(Modified skin scores)을 시행하여 골수유래줄기세포 및 성장인자 적용 후 치유 정도를 평가하였다. 이후 연조직 병변은 조직염색으로 평가하였다.

[연구 결과]

방사선 조사 후 16일 이내에 방사선 조사부위의 40% 이상에서 궤양이 발생하였으며 3 주 경과 후 궤양은 방사선 조사면적의 50%가 넘는 최대 크기에 도달 하였다. 골수유래줄기세포 단독 적용군과 혈소판유래 성장인자 단독 적용군에서는 유의할 치유 효과가 관찰되지 않았다. 골수유래줄기세포 및 혈소판유래 성장인자 혼합 적용군에서는 적용 후 2주간 궤양 면적 비율에 있어서 대조군 대비 유의한 감소가 관찰되었다. 조직염색 결과 혈소판유래 성장인자 단독 적용군 및 골수유래줄기세포 및 혈소판유래 성장인자 혼합 적용군에서 대조군 대비 고형질의 교원섬유가 진피층 전부위에서 관찰되었다.

Part II. 방사선유발 골괴사에 대한 효과

[재료 및 방법]

비폐쇄형 피부클램프를 사용하여 백서의 체부와 내장을 보호하고 image guided stereotactic irradiator를 사용하여 하악골에 방사선 조사를 시행하였다. 조사거리는 100 cm로 일정하였으며 30Gy의 방사선을 백

서의 우측 하악 동일부에 조사하였다. 방사선 조사 일주일 후 우측 하악골의 모든 구치에 대해 발거술 및 동일한 크기의 외상부 형성을 시행하였다. 백서는 하이드로젤 복합체의 적용시기에 따라 두 군으로 임의로 분류되었다(각 그룹당 n=25). 1군에서는 외상형성 직후 외상부에 골수유래줄기세포 혹은 골형성단백질-2를 포함한 하이드로젤을 적용하고 4주간 경과관찰 하였다. 2군에서는 외상부 형성 후 4주 경과 후 방사선골괴사의 발생을 확인 한 후 골수유래줄기세포 혹은 골형성단백질-2를 포함한 하이드로젤을 적용하고 4주간 경과관찰 하였다. 각 실험군은 대조군 (n=5), 하이드로젤 단독 적용군(n=5), 골수유래줄기세포 2 x 10^4 를 포함한 하이드로젤 적용군 (n=5), 10 μg의 골형성단백질-2를 포함한 하이드로젤 적용군 (n=5), 골수유래줄기세포 2 x 10^4 및 10 μg의 골형성단백질-2 혼합하여 포함된 하이드로젤 적용군(n=5)로 구성되었다. 골조직 치유를 평가하기 위하여 미세초첨 컴퓨터단층촬영을 시행하여 각 그룹간 비교를 하였다. 방사선 조사를 받지 않고 외상부 형성만 시행받은 백서에 대해서 음성대조군으로 비교 분석 하였다.

[연구 결과]

1 군에서는 골형성단백질-2가 포함된 하이드로젤 적용군에서 골부피(bone volume, BV) 및 골밀도(bone mineral density, BMD)의 유의한 증가가 관찰되었으나 골수유래줄기세포를 적용하는 경우 대조군 대비 평가 항목에서 유의한 차이가 관찰되지 않았다. 2 군의 모든 개체에서 방사

선골괴사가 발생한 것이 관찰되었다. 2군에서는 골수유래줄기세포 및 골형성단백질-2가 혼합 포함된 하이드로젤 적용시 하이드로젤 단독 적용군 및 대조군 대비 골부피 및 골밀도의 유의한 증가가 관찰되었다. 1군에서 골형성단백질-2가 포함된 하이드로젤을 적용한 군(6.29 ± 1.63%) 은 2군에서 골형성단백질-2가 포함된 하이드로젤을 적용한 군(5.71 ± 0.94%)에 비해 골밀도가 유의미하게 높은 것으로 관찰되었다.

결론

백서의 방사선유발 연조직 궤양에서 골수유래 줄기세포와 혈소판유래 성장인자 혼합 적용시 유의한 치유증대 효과가 관찰되었다. 백서에서 방사선 조사 후 형성한 외상부 골조직의 치유는 치조골외상부 형성 직후 골형성단백질-2를 포함한 하이드로젤 적용시 치유 증대가 관찰되었다. 반면 방사선골괴사 발생 이후 적용시에는 골수유래줄기세포 및 골형성단백질-2의 혼합 포함된 하이드로젤 적용시 골조직의 치유 증대 효과가 관찰되었다.

주 요 어: 골수유래 줄기세포, 혈소판유래성장인자, 골형성단백질-2, 방사선골괴사, 백서

학 번: 2012-30615